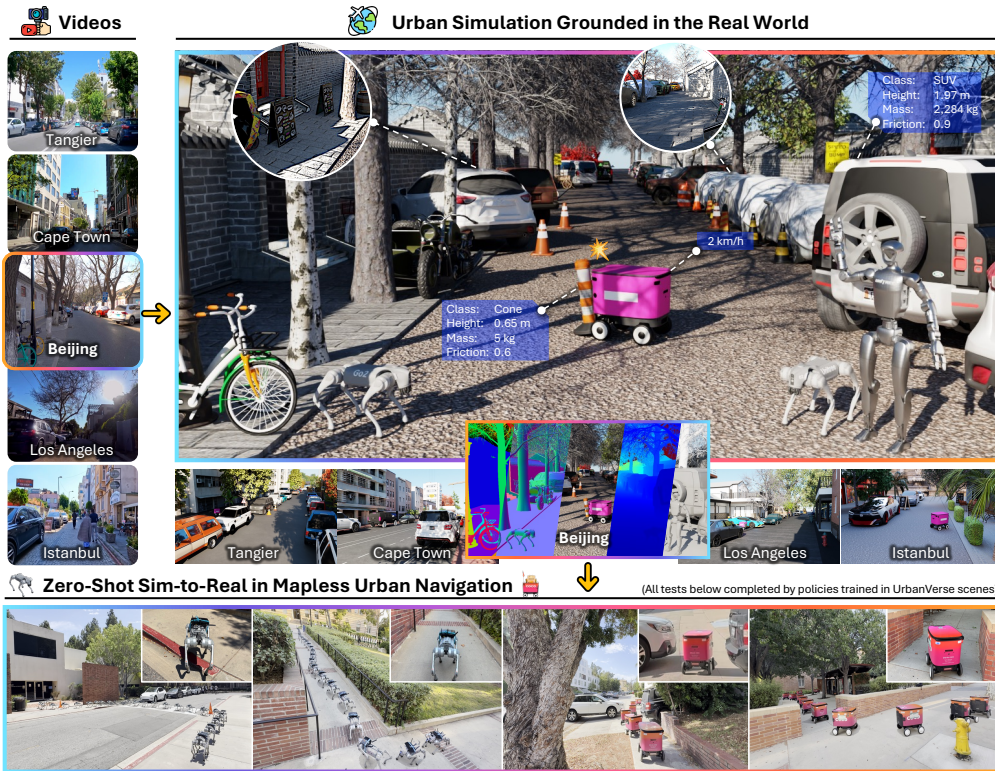


URBANVERSE: SCALING URBAN SIMULATION BY WATCHING CITY-TOUR VIDEOS

000
001
002
003
004
005 **Anonymous authors**
006 Paper under double-blind review
007



008
009
010
011
012
013
014
015
016
017
018
019
020
021
022
023
024
025
026
027
028
029
030
031
032
033
034
035
036
037
038
039
040
041
042
043
044
045
046
047
048
049
050
051
052
053
Figure 1: **UrbanVerse** system converts real-world urban scenes from city-tour videos into physics-aware, interactive simulation environments, enabling scalable robot learning in urban spaces with real-world generalization.

ABSTRACT

Urban embodied AI agents, ranging from delivery robots to quadrupeds, are increasingly populating our cities, navigating chaotic streets to provide last-mile connectivity. Training such agents requires diverse, high-fidelity urban environments to scale, yet existing human-crafted or procedurally generated simulation scenes either lack scalability or fail to capture real-world complexity. We introduce **UrbanVerse**, a data-driven real-to-sim system that converts crowd-sourced city-tour videos into physics-aware, interactive simulation scenes. UrbanVerse consists of: (i) *UrbanVerse-100K*, a repository of 100k+ annotated urban 3D assets with semantic and physical attributes, and (ii) *UrbanVerse-Gen*, an automatic pipeline that extracts scene layouts from video and instantiates metric-scale 3D simulations using retrieved assets. Running in IsaacSim, UrbanVerse offers 160 high-quality constructed scenes from 24 countries, along with a curated benchmark of 10 artist-designed test scenes. Experiments show that UrbanVerse scenes preserve real-world semantics and layouts, achieving human-evaluated realism comparable to manually crafted scenes. In urban navigation, policies trained in UrbanVerse exhibit scaling power laws and strong generalization, improving success by +6.3% in simulation and +30.1% in zero-shot sim-to-real transfer comparing to prior methods, accomplishing a 300 m real-world mission with only two interventions. We invite readers to explore our anonymous [Demo Page](#) and [Documentation Page](#).

054

1 INTRODUCTION

055
 056 Today’s urban spaces have emerged as key arenas for the rise of micromobility systems (Oeschger
 057 et al., 2020). Small, lightweight Embodied AI (E-AI) agents (Zhang et al., 2024), such as wheeled
 058 delivery robots, quadrupeds, and humanoids, are increasingly navigating city streets to provide
 059 last-mile transportation and urban services. These mobile robots are reshaping the dynamics of city
 060 streets by improving logistical efficiency and reducing carbon emissions. Yet, the environments
 061 they operate in are often highly cluttered, with street infrastructure, sidewalks frequently blocked by
 062 parked cars, and narrow passageways, all of which pose significant challenges for E-AI agents to
 063 generalize across diverse real-world settings.

064 In efforts to improve generalizability, data scaling has been validated in both vision (Radford et al.,
 065 2021) and language (Kaplan et al., 2020), where large and diverse web corpora consistently lead to
 066 better generalization. In contrast, current urban navigation datasets remain limited in both *scale* and
 067 *quality*. Collecting high-quality data through human demonstrations in public spaces (e.g., sidewalk
 068 traversing) is unsafe, labor-intensive, and often impractical, and thus cannot scale (Shah et al.,
 069 2023). Passive real-world data, such as city-tour videos shared daily on social media like YouTube,
 070 captures diverse environments but lacks associated action labels. Moreover, both types of data are
 071 *non-interactive* and lack *causal action–effect* dynamics, which are crucial for robust real-world
 072 decision-making. Thus, urban simulators (Wu et al., 2025a) have emerged as a compelling alternative,
 073 offering interactive and virtually unlimited scenes for E-AI training. Yet, current simulators either
 074 rely on hand-crafted scenes (Dosovitskiy et al., 2017) or procedurally generated layouts defined by
 075 hard-coded rules (Wu et al., 2025a;b). The former lacks scalability, while the latter produces rigid,
 076 template-driven scenes that deviate from real-world distributions, such as randomly parked scooters
 077 or cars. However, simply increasing its quantity will lead to sustained generalization if the data does
 078 not faithfully reflect real-world distributions. This issue prompts the central question of this work:
 079 *Can we build realistic, interactive urban scenes from real-world videos for scalable robot navigation?*

080 To address this question, we propose **UrbanVerse**, a data-driven real-to-sim system that bridges
 081 the gap between synthetic simulators and the complex, real-world streets. As shown in Fig. 1
 082 (top), UrbanVerse reconstructs interactive urban scenes with real-world distributional fidelity from
 083 worldwide city-tour videos (walking or driving), enabling the training of “street-smart” urban agents.
 084 At its core, UrbanVerse reconstructs *digital cousin* (Dai et al., 2024) scenes, by mapping a 2D scene
 085 to a 3D simulation-ready virtual world, with layouts, semantics, and physics aligned to real-world
 086 statistics. *This combines the diversity of real data with the interactivity of simulation*, enabling
 087 unlimited scene generation while preserving street-level distributions. UrbanVerse builds on two
 088 complementary pillars. The first is **UrbanVerse-100K** (Fig. 2), a curated repository of 102,530
 089 high-quality metric-scale urban object assets, 306 skyboxes, and 288 ground materials for roads and
 090 sidewalks. Each asset is organized within a three-level urban ontology and annotated with 33 semantic,
 091 affordance, and physical attributes (e.g., mass, friction), forming the foundation for open-world,
 092 physics-ready scene construction. The second is **UrbanVerse-Gen** (Fig. 4), an automatic pipeline
 093 that accurately distills semantics, layouts, ground appearance, and sky from videos into an urban
 094 scene graph representation, retrieves matched assets from UrbanVerse-100K, and instantiates multiple
 095 digital cousin simulation scenes in IsaacSim (NVIDIA, 2025). Using YouTube city-tour footage
 096 spanning 24 countries across six continents, UrbanVerse produces a library of 160 simulation scenes
 097 with real-world street distributional fidelity ready for E-AI training. Together, we also introduce a 3D
 098 artist-designed set of 10 realistic urban scenes as test-only environments for closed-loop evaluation.

099 UrbanVerse is evaluated through both scene generation quality assessment and its applicability to
 100 urban E-AI policy learning. Validated on 45 video sequences from KITTI-360 (Liao et al., 2022),
 101 our approach achieves high-fidelity scene reconstruction, recovering object semantics with 93.0%
 102 accuracy and localizing objects within 1.4 m error over 198.7 m scene horizon. Building on this real-
 103 world distributional fidelity, we train mapless urban navigation policies using a 160-scene simulation
 104 library generated by UrbanVerse. We show that data scaling *power-law* emerges when training on our
 105 high-fidelity scenes, enabling simple policies to generalize to diverse, unseen urban spaces. Deployed
 106 across 16 real-world streets on two embodiments (a wheeled robot and a quadruped) in a zero-shot
 107 manner, policies trained on UrbanVerse scenes consistently outperform state-of-the-art navigation
 108 foundation models, reaching up to 89.7% success in sim-to-real transfer. Finally, our policy completes
 109 a 337 m long-horizon mission in public spaces with only two human interventions. All assets, scenes,
 110 and code of UrbanVerse will be *open-sourced* to accelerate embodied AI research.

108	Simulator	Scene Creation	Layout Realism	Scene Diversity	Asset Physics	# Object Classes	# Object Assets	# Sky Maps	# Ground Materials	# Robot Types	Dynamic Factors	Training Paradigms	Embodied Tasks
109	CARLA	Hand Crafted	Realistic	15 Scenes	✓	106	935	5	30	1	Dynamic agents Weather	RL, IL VLA	Navigation, VQA
110	MetaUrban	Procedural Generation	Unrealistic	7 Templates	✗	39	10,000	1	5	1	Dynamic agents	RL, IL	Navigation
111	UrbanSim	Procedural Generation	Unrealistic	6 Templates	✗	39	15,000	1	8	10	Dynamic agents	RL, IL	Navigation
112	UrbanVerse	Auto Real2Sim Data-driven	Realistic	$+\infty$	✓	667	102,530	306	288	20	Dynamic agents, Illumination Ground appearance	RL, IL VLA	Navigation, VQA Mobile Manipulation

Table 1: **Systematic comparison of UrbanVerse with existing urban embodied-AI simulators.**

2 RELATED WORK

Urban Navigation. Deep reinforcement learning (Mirowski et al., 2016) has demonstrated strong potential for goal-based mapless urban navigation by removing the dependency on pre-built maps (Chaplot et al., 2020). Recent advances have introduced vision-based navigation foundation models (Shah et al., 2023; Sridhar et al., 2024; Hirose et al., 2025), which leverage cross-sensor capabilities and large-scale offline vision data to improve generalization across robot platforms and camera setups. A major limitation of these approaches, however, is the lack of environmental interaction in the training data. As we demonstrate in Sec. 4.3, this results in poor obstacle avoidance (Liu et al., 2025). S2E (He et al., 2025) tackles this issue by training in interactive simulation scenes, rather than relying on passive data for path-following, and achieves real-world obstacle avoidance. In this work, we extend both coverage and realism by training vision-based position-goal navigation policies in our real-world grounded UrbanVerse scenes, leading to improved robustness and generalization.

Urban Embodied AI Simulators. Mainstream simulators focus either on *indoor* environments (Kolve et al., 2017; Li et al., 2023a) or on *driving* domains centered on roads and highways (Kothari et al., 2021; Li et al., 2022), with only CARLA (Dosovitskiy et al., 2017) extending to city neighborhoods but relying on non-scalable, hand-crafted scenes (15 in total). The rise of *micromobility* (Abduljabbar et al., 2021) agents, such as e-scooter or delivery robots, has motivated the development of *urban* simulators like MetaUrban (Wu et al., 2025a) and UrbanSim (Wu et al., 2025b), which share our goal of modeling richer city spaces. However, these simulators face three key limitations: *i*) *layout realism*: procedurally generated scenes deviate from real-world distributions; *ii*) *asset diversity*: limited object categories; *iii*) *physics annotation*: objects lack physical properties and remain static props. **We provide a functional comparison between UrbanVerse and existing urban simulators in Tab. 1.** Building upon UrbanSim simulation platform, we address these gaps with our real-world grounded scene creation pipeline and a semantically-rich, physics-annotated asset library.

Simulation Scene Creation. Automating scene creation for E-AI learning has traditionally relied on either enhancing procedural generation rules (Deitke et al., 2022; Li et al., 2023b; Yang et al., 2024; Wu et al., 2025a;b) or using high-precision 3D scans to replicate real-world environments (Deitke et al., 2023a; Huang et al., 2025; Yu et al., 2025). More recently, 3D Gaussian Splatting (3DGS) methods like OmniRe (Chen et al., 2024) and Vid2Sim (Xie et al., 2025) reconstruct 3DGS digital twin environments from RGB videos for coarse simulation. **However, current 3DGS-based digital twins are designed for one-to-one reconstruction and produce a single fused radiance field without complete geometry, object instances, semantics, or physical attributes, making them unsuitable for editing, interaction, or physics-based simulation.** Our work shares conceptual similarities with digital cousin approaches (Dai et al., 2024; Maddukuri et al., 2025; Melnik et al., 2025), which generate multiple virtual *indoor* scenes from a *calibrated RGB image* while preserving key semantics, geometry, and layout to improve manipulation policies. In contrast, UrbanVerse constructs large-scale, street-level urban digital cousin scenes from *uncalibrated RGB videos*.

3 METHODOLOGY

To convert worldwide city-tour videos into physics-aware simulations, two indispensable elements are required: *i*) a large-scale 3D asset database with physical annotations that match the magnitude of real-world semantic richness and appearance diversity, and *ii*) an automated open-vocabulary pipeline that extracts semantic and spatial layouts from any uncalibrated videos to generate simulation scenes. To this end, in Sec. 3.1, we first describe the data collection and semi-automatic annotation pipeline in UrbanVerse for building the **UrbanVerse-100K** database. Next, in Sec. 3.2, we present **UrbanVerse-Gen**, our automated pipeline that extracts detailed scene representations from videos



Figure 2: Example instances from our large-scale urban asset database **UrbanVerse-100K**. Assets range from 0.03 m crushed can to a 200 m skyscraper, all annotated to metric scale; *note the realistic relative scales between objects*, with road and sidewalk materials and sky maps ensuring realistic ground appearance and illumination. to ground simulated scene generation. Finally, in Sec. 3.3, we show how UrbanVerse leverages crowd-sourced videos to construct a large-scale scene library for policy learning and testing.

3.1 URBANVERSE-100K ASSET DATABASE

UrbanVerse-100K is a large-scale, high-quality 3D asset database designed for urban simulation and beyond. To comprehensively model real-world scenes, we require not only a vast collection of on-ground 3D object assets but also diverse materials to render ground surfaces (*e.g.*, cobblestone sidewalks or snowy roads) and realistic lighting conditions across different times of day. Each of these significantly influences robot perception and interactivity. For this, as shown in Fig. 2, UrbanVerse-100K comprises three collections: (*i*) *Object*: 102,530 GLB objects spanning 667 categories, each annotated with 33 semantic, physical, and affordance attributes in true metric scale; (*ii*) *Ground*: 288 photorealistic PBR materials (98 road, 190 sidewalk) for ground plane texturing; and (*iii*) *Sky*: 306 HDRI sky maps for realistic global illumination and immersive 360° backgrounds. We next outline the collection and annotation strategies for UrbanVerse-100K, with additional details in App. C.

Object Collection. The recent development of large-scale 3D object repositories (Deitke et al., 2023b), such as Objaverse (Deitke et al., 2023c), provides valuable resources for constructing simulation scenes. However, due to their web-crawled nature, these repositories suffer from several critical issues: (*i*) most assets are *unrelated* to urban environments; (*ii*) many assets are *corrupted* (*e.g.*, missing textures, incomplete 3DGS reconstructions, or paper-thin geometry); (*iii*) assets often have *non-metric* scales, with examples such as a cucumber being as large as a car; and (*iv*) assets lack semantic and physical attribute annotations. Fig. 18 and Fig. 19 in the appendix illustrate these issues. To this end, we curate a high-quality urban subset from the 800K noisy 3D assets in the Objaverse dataset (Deitke et al., 2023c) through a three-stage semi-automatic pipeline. First, we build a Three.js-based asset viewer interface (Fig. 15) and employ human annotators to efficiently filter out corrupted or low-quality assets. After filtering, we retain 158K high-quality assets. Next, we build a *three-level* urban ontology derived from the OpenStreetMap tag structure (Bennett, 2010) and expanded with categories from driving and scene understanding datasets (Zhou et al., 2017; Cordts et al., 2016; Caesar et al., 2020; Gupta et al., 2019; Kuznetsova et al., 2020), resulting in 667 leaf-level categories. Next, each asset is classified into a leaf category using CLIP (Radford et al., 2021) on its thumbnail, followed by manual verification to remove non-urban items (*e.g.*, game weapons, spaceships) and correct misclassifications, yielding our final curated set of objects. Lastly, we leverage the world knowledge of GPT-4.1 (OpenAI, 2025) to

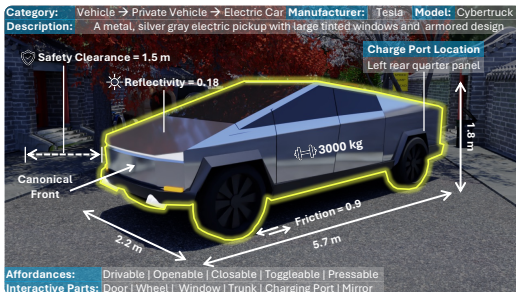


Figure 3: Example of annotated object attributes.

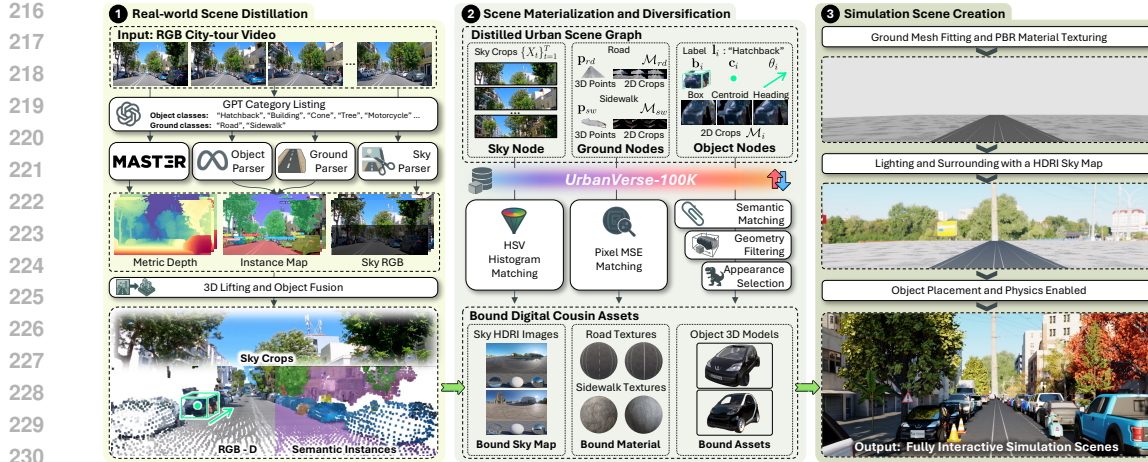


Figure 4: Overview of the UrbanVerse-Gen pipeline. Figure better seen at magnification.

annotate each asset with semantic, affordance, and physical attributes (e.g., size, mass). We prompt it with the object thumbnail and four rotated snapshots. Fig. 3 shows an example of few annotated attributes. Using the annotated size and front-view, as displayed in Fig. 2 (left), we standardize all assets in our database to metric scale and a consistent orientation.

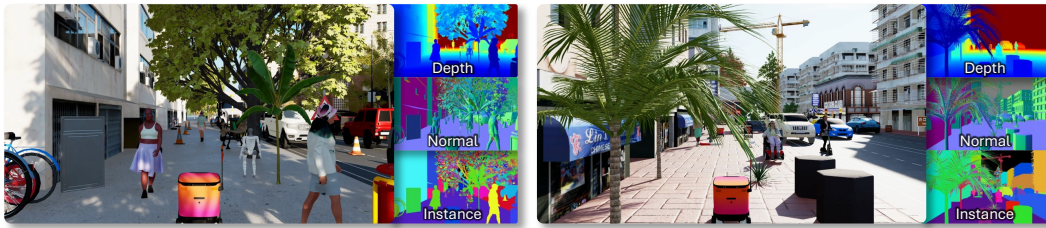
Ground and Sky Collections. To provide the simulated ground plane with realistic and diverse appearances, we collect 4K-quality PBR road and sidewalk materials from free-licensed repositories (FreePBR, 2025; AmbientCG, 2025), each with a thumbnail and spanning a wide range of conditions, as shown in Fig. 2 (middle). For lighting, we gather artist-designed HDRI sky maps (Fig. 2 (right)) for urban settings from PolyHaven (2025), each accompanied by a rendered thumbnail and description. These maps enable image-based lighting, providing realistic global illumination with precise control over color, intensity, and direction, while also supplying immersive background.

3.2 URBANVERSE-GEN SCENE CONSTRUCTION PIPELINE

With our richly annotated asset database, we design **UrbanVerse-Gen**, an automatic open-vocabulary pipeline capable of extracting real-world 3D scene layouts from uncalibrated RGB city-tour videos and generating fully interactive simulations. To structure a scene, we first introduce a unified 3D urban scene graph $\mathcal{V} = \langle \mathcal{O}, \mathcal{G}, \mathcal{S} \rangle$ that encodes: (i) **object nodes** (e.g., cars, buildings) with category, location, orientation, and appearance; (ii) **ground nodes** (road/sidewalk) with spatial extent and appearance; and (iii) **sky node** capturing illumination and distant background. Distilled from real-world videos, this graph serves as a compact *blueprint* for guiding simulation scene generation.

Overview. As shown in Fig. 4, UrbanVerse-Gen operates in three stages: (1) *distillation*, where object semantics and 3D layout, ground composition (road/sidewalk) and appearance, lighting, and distant background are extracted from the input video into a unified scene graph representation; (2) *materialization and diversification*, where multiple digital cousin assets from UrbanVerse-100K are matched and bound to each graph instance; and (3) *generation*, where object, ground, and sky instances are assembled with their extracted spatial information into physically plausible scenes. We detail each stage below. Further technical specifics are in App. E.

Real-World Scene Distillation. To accurately parse semantics and estimate 3D layouts from uncalibrated open-world videos, we design a distillation module that integrates 2D open-vocabulary foundation models with SfM through 3D lifting. Given an RGB city-tour video $\mathcal{I} = \{I_t^{\text{rgb}}\}_{t=1}^T$, we sample every third frame and query GPT-4.1 (OpenAI, 2025) to enumerate visible categories and form a candidate vocabulary. The video is lifted to metric 3D by estimating depth, intrinsics, and SE(3) poses using MASt3R (Leroy et al., 2024). With these semantic and geometric estimates, we assemble an open-vocabulary object parser using YoloWorld (Cheng et al., 2024) and SAM 2 (Ravi et al., 2024) to obtain per-frame instance masks, which are lifted to metric 3D. Identical detections are fused across frames by semantic similarity and point-cloud overlap, yielding N persistent object nodes $\mathcal{O} = \{\mathbf{o}_i = \langle \mathbf{l}_i, \mathbf{c}_i, \mathbf{b}_i, \theta_i, \mathcal{M}_i \rangle\}_{i=1}^N$, where \mathbf{l}_i is the category, \mathbf{c}_i the centroid, \mathbf{b}_i the oriented 3D box, θ_i the yaw, and $\mathcal{M}_i = \{\mathbf{m}_{i,j}\}_j$ the 2D object crops. In parallel, we segment



270
271
272
273
274
275
276
277
278 Figure 5: **Diverse dynamic agents in UrbanVerse scenes.** Two example scenes populated with pedestrians,
279 cars, wheelchair users, and scooter riders, shown across multiple observation modalities.

280 road and sidewalk using a panoptic Mask2Former ground parser (Cheng et al., 2022) trained on
281 Cityscapes (Cordts et al., 2016), lift and fuse results into metric point clouds \mathbf{p} , and define ground
282 nodes $\mathcal{G} = \{\langle \text{road}, \mathbf{p}_{rd}, \mathcal{M}_{rd} \rangle, \langle \text{sidewalk}, \mathbf{p}_{sw}, \mathcal{M}_{sw} \rangle\}$, where \mathcal{M} preserves ground masks. Finally,
283 the sky parser captures global illumination and distant background by cropping the upper half of each
284 frame, stored in the sky node as $\mathcal{S} = \{X_t\}_{t=1}^T$.

285 **Scene Materialization and Diversification.** With the distilled scene graph, our goal is to materialize
286 each instance using *digital-cousin* assets from UrbanVerse-100K that are semantically aligned,
287 geometrically consistent, and visually faithful yet diverse, enabling varied appearances for stronger
288 policy generalization. To meet these requirements, we retrieve k_{cousin} assets for each object node
289 $\mathbf{o}_i \in \mathcal{O}$ through three corresponding steps: (i) *semantic matching* selects the best-matched asset
290 category via CLIP similarity (Radford et al., 2021) with its label \mathbf{l}_i ; (ii) *geometry filtering* ranks
291 candidates within that category by minimal Bounding Box Distortion (mBB) between \mathbf{b}_i and
292 candidate boxes, retaining the top 1,000; (iii) *appearance selection* re-ranks these candidates using
293 DINOv2 similarity (Oquab et al., 2023) between \mathcal{M}_i and asset thumbnails, keeping the top- k_{cousin} as
294 final matches. For ground nodes, we retrieve k_{cousin} PBR materials by comparing pixel-wise MSE
295 between road/sidewalk crops $\mathcal{M}_{rd}/\mathcal{M}_{sw}$ and rendered thumbnails. For the sky node, we select
296 k_{cousin} HDRIs by matching HSV histograms of sky crops $\{X_t\}$ to HDRI thumbnails, reproducing
297 illumination and distant background.

298 **Simulation Scene Creation.** Finally, we instantiate the materialized graph into k_{cousin} simulated
299 scenes in UrbanSim (IsaacSim backend) by: (i) *ground fitting and texturing*, where road and sidewalk
300 planes are fitted from $\mathbf{p}_{rd}/\mathbf{p}_{sw}$, sidewalks are elevated by 15 cm, and surfaces are textured with the
301 selected PBR materials; (ii) *lighting and surroundings*, where a matched HDRI sky map is used as
302 both a dome light source and a spherical environment to provide realistic skies and distant context;
303 (iii) *object placement*, where each object is positioned at its centroid \mathbf{c}_i , aligned to the canonical front
304 and heading θ_i , and adjusted to avoid penetrations. We then assign annotated physical parameters
305 (e.g., mass, friction) and enable rigid-body dynamics, producing stable, interactive scenes. With
306 metrically scaled assets from UrbanVerse-100K aligned to extracted layouts, the resulting scenes are
307 true-to-scale, grounded in real-world layouts, and ready for E-AI agents to explore.

308 **Interactive Dynamic Agent Population.** UrbanVerse also supports dynamic agents such as pedes-
309 trians, cars, wheelchair users, and scooter riders. Following UrbanSim (Wu et al., 2025b), we use a
310 GPU-accelerated ORCA-based planner (Van Den Berg et al., 2011) to populate scenes with agents
311 that move realistically and interact with the robot. For each scene, we build a 2D occupancy map,
312 sample start-goal pairs, and compute collision-free paths; agents then continuously adjust their veloc-
313 ities during simulation for smooth, collision-aware motion. As shown in Fig. 5, this scene-agnostic
314 mechanism enables diverse dynamic agents across all UrbanVerse environments.

315 3.3 URBANVERSE SCENE LIBRARY

317 **UrbanVerse Scene Library Construction.** Using UrbanVerse, we build a *training* library of 160
318 simulation scenes grounded in real-world distribution. We have collected 32 city-tour videos from
319 YouTube under Creative Commons License, spanning 7 continents, 24 countries, and 27 cities. Each
320 3-min clip is distilled into a layout-grounded scene using our UrbanVerse-Gen and expanded into
321 $k_{\text{cousin}} = 5$ digital cousin variants, yielding $5 \times 32 = 160$ scenes. See construction details in App. D.2.

322 **UrbanVerse Benchmark.** Further, to enable closed-loop evaluation, we construct a benchmark that
323 comprises: (i) *AutoBench*, 10 scenes automatically generated from hold-out city-tour videos using

324
325
326
327
328
329
330
331
332
333
334
335
336
337
338
339
340
341
342
343
344
345
346
347
348
349
350
351
352
353
354
355
356
357
358
359
360
361
362
363
364
365
366
367
368
369
370
371
372
373
374
375
376
377
Figure 6: **Urban embodied-AI tasks supported by the UrbanVerse simulation platform.**

UrbanVerse-Gen; and (ii) *CraftBench*, 10 artist-designed scenes reserved for test-only evaluation. As shown in Fig. 22 in appendix, CraftBench spans diverse scenarios, layouts, cultural context, and safety-critical edge cases. To avoid bias, designers had no access to our assets and scenes.

UrbanVerse Tasks. In this work, we focus on *urban navigation* as the primary case study in our experiments because it most clearly demonstrates the benefits of UrbanVerse’s realistic layouts and asset distributions. However, all assets in UrbanVerse include semantic labels, physical parameters, and affordance tags, enabling a wide range of urban embodied tasks. As the few examples illustrated in Fig. 6, UrbanVerse naturally supports multi-agent interaction, mobile manipulation, and expert data collection for imitation learning, opening broader research opportunities.

4 EXPERIMENTS

We evaluate UrbanVerse on three aspects: (i) **scene construction capability**, assessing fidelity and quality of scenes constructed from real-world videos (Sec. 4.1); (ii) **scaling capability**, examining whether training on UrbanVerse scenes follows scaling laws that improve policy generalization (Sec. 4.2); and (iii) **sim-to-real transfer capability**, testing whether policies trained in UrbanVerse enable robust and stable transfer to real-world environments (Sec. 4.3).

Policy learning for mapless urban navigation. In our study, following Wu et al. (2025b), we focus on RL to exploit scene interactivity, and study the task of *position-goal urban navigation*: the agent starts from a known ground-plane pose, receives a goal and waypoints sampled every 5 m from GPS projected to a local metric frame, and must learn a policy to reach the goal within a distance tolerance while avoiding collisions and staying on traversable surfaces. Using the 160-scene UrbanVerse library, we train vision-only navigation policies using PPO (Schulman et al., 2017) to show the effectiveness of our real-world grounded simulation scenes. During training, we load 16 different scenes at a time and repeat each scene 4–6 times depending on the available GPU memory. The set of scenes is changed every 100 RL episodes to expose the policy to diverse environments. In both training and testing, the agent is provided with *only RGB* observation, its relative position to the goal, *without* access to the global map. See model architecture and training details in App. J.3.

4.1 SCENE CONSTRUCTION FIDELITY AND QUALITY

Scene fidelity evaluation. We first evaluate whether UrbanVerse can faithfully recover scene semantics and layouts from video. Using 45 KITTI-360 (Liao et al., 2022) sequences (average length 198.7 m) of residential and city streets, we generate digital cousin scenes with UrbanVerse-Gen. Scene reconstruction fidelity is measured by comparing the nearest digital-cousin scene, built with top-1 matched assets, against ground-truth annotations: semantic fidelity by the proportion of correctly preserved categories; layout fidelity by per-object pose errors (L_2 distance and orientation difference); geometric fidelity by bounding-box volume difference; and overall recovery by 3D detection mAP25 (Kumar et al., 2024). Appearance fidelity cannot be directly measured since real-world asset replicas are unavailable. Instead, we input walkthrough videos of ten simulated CraftBench scenes into UrbanVerse-Gen and report the proportion of objects whose 3D models are exactly retrieved. For comparison, we evaluate two SfM models (VGGT (Wang et al., 2025) and our default MASt3R) and two open-vocabulary parsers (GroundedSAM2 (Ren et al., 2024) and our default YoWorldSAM2, combining YoloWorld with SAM2). Lastly, we present side-by-side comparisons of city-tour videos and their reconstructed scenes in Fig. 7.

Quantitatively, Tab. 2 shows that the MASt3R with our YoWorldSAM2 parser yields the best overall results, which we adopt as UrbanVerse’s default. With this setup, 93.1% of object categories are correctly preserved; reconstructed objects deviate by only 1.4 m in position, 19.8° in orientation, and 0.8 m³ in volume. Asset retrieval achieves 75.1% accuracy, indicating effective matching of

SfM	Scene Parser	Cat. (%)↑	Dist. (m) ↓	Ori. (°) ↓	Scale (m ³) ↓	mAP25↑	Ast. (%)↑
VGTT	GroundedSAM2	88.2	2.4	21.5	1.5	7.5	67.5
	YoWorldSAM2	91.5	2.1	20.1	1.3	9.4	70.6
MASt3R	GroundedSAM2	86.1	2.1	19.9	1.1	24.3	68.5
	YoWorldSAM2	93.1	1.4	19.8	0.8	28.2	75.1

Table 2: **Scene reconstruction fidelity evaluation of nearest digital-cousin generation.** We report average results on KITTI-360, including: Category recovery (Cat.), the fraction of correctly categorized objects; Distance (Dist.), Orientation (Ori.), and Scale, the mean differences in centroid position, heading, and volume between recovered and ground-truth bounding boxes; and 3D detection mAP. Asset recovery (Ast.), the fraction of correctly retrieved objects evaluated from CraftBench scene videos, is also reported.



Figure 7: **Qualitative scene generation results of UrbanVerse.** Scenes generated from Cape Town (left) and Morocco (right) city-tour videos in our library. Highlighted details are shown in the circled areas. See Fig. 20 in the Appendix for additional qualitative results.

visually similar 3D assets from our database. Qualitatively, Fig. 7 shows that UrbanVerse produces physically plausible scenes that preserve fine object placement details from the original videos, such as cranes located in the distance or motorcycles parked along the roadside. Given the long horizon length of the evaluated street scenes, these results demonstrate that UrbanVerse can faithfully capture real-world semantics and layout distributions from casual city-tour videos, enabling the generation of high-fidelity simulated scenes that reflect real-world street distribution.

Human Evaluation of Scene Quality. We evaluate whether UrbanVerse scenes align with human impressions of everyday streets through two user studies with 32 undergraduates. In the first comparative study, 100 UrbanVerse scenes sampled from our library are paired with 100 UrbanSim’s procedurally generated (PG) scenes generated from the same UrbanVerse-100K assets. Participants view shuffled overview images and choose which scene is better (or equally good) in terms of object diversity, layout coherence, and overall realism. In the second study, participants rate the overall realism of 30 scenes, 10 from UrbanVerse, 10 from PG, and 10 artist-designed oracles from CraftBench, by watching 360° walkthrough videos and scoring them on a 1–5 scale. Further details are provided in App. K.

As shown in Fig. 8 (a–c), participants consistently preferred UrbanVerse over PG, with more than 70% favoring it across Object Diversity, Layout Coherence, and Overall Realism. In the second study, the human ratings of artist-designed scenes (4.08/5.00) in Fig. 8 (d) suggest that even hand-crafted scenes are imperfect, underscoring the challenge of creating highly realistic outdoor environments. Given this difficulty, the 3.58/5.00 score of UrbanVerse scenes is satisfactory for an automated approach.

4.2 SCALING URBANVERSE FOR POLICY GENERALIZATION

We next examine the scaling properties of using the UrbanVerse 160-scene library for policy generalization in mapless urban navigation on a wheeled robot. We first study how the number of training layouts influences generalization, then analyze the effect of expanding each layout with more digital cousins. Policy performance is measured by success rate (SR), route completion (RC), and collision times (CT), with all evaluations conducted in *unseen* environments from AutoBench and CraftBench. We provide detailed experimental setups and metric definitions in App. J.

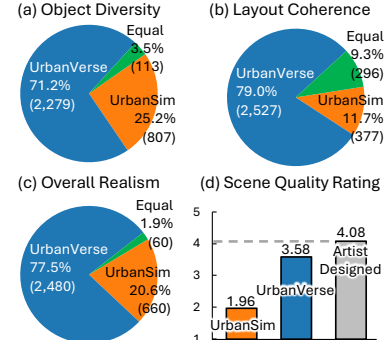


Figure 8: **Human evaluation results.**

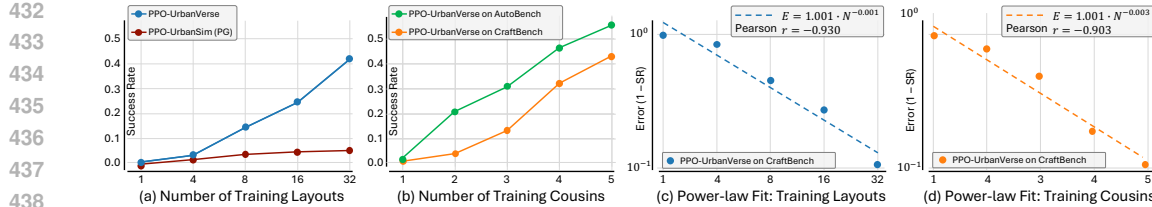


Figure 9: Generalization by scaling training layouts and digital cousins per scene.

Scaling with more unique layouts. We fix the number of cousins per layout and vary the number of unique layouts. From the 160-scene UrbanVerse library, we select 32 unique layouts (each from a distinct city-tour video), each expanded with five cousins. Training sets are constructed with $N \in \{1, 8, 16, 32\}$ layouts, corresponding to 5, 40, 80, and 160 scenes. For comparison, we train policies on matched PG scenes in UrbanSim with identical layout counts and per-layout variants. Policies are then evaluated on the 10 CraftBench scenes with five runs per scene. As shown in Fig. 9 (a), increasing the number of UrbanVerse layouts consistently improves generalization, with success rates rising sharply as coverage expands. The flat slope at small N highlights how limited layout diversity constrains generalization. In contrast, policies trained on PG layouts show very limited improvement, indicating that hard-coded templates lack the diversity needed to scale.

Scaling with more digital cousins. We fix the number of unique layouts and vary the number of digital cousins per layout. Using 32 layouts, we select $m \in \{1, 2, 3, 4, 5\}$ top-ranked cousins, yielding training sets of 32–160 scenes. Policies trained on these sets are evaluated on 10 AutoBench scenes and 10 CraftBench scenes. As shown in Fig. 9 (b), increasing the number of cousins consistently further boosts success rate, confirming that intra-layout diversity complements inter-layout diversity to reinforce generalization. Performance is overall higher on AutoBench, reflecting distributional familiarity with scenes generated by the same pipeline, while the lower scores on CraftBench highlight the difficulty of artist-designed environments. Notably, the narrowing gap between the two testbeds indicates that greater per-layout diversity improves robustness to distribution shift.

Validating scaling power laws. We next validate whether performance gains follow a power-law scaling relationship (Lin et al., 2025b). Defining test error as $E = 1 - SR$ and training scale as N (number of layouts or cousins), a power law holds if $E = \beta N^{-\alpha}$, which becomes linear after log transform: $\log E = -\alpha \log N + \log \beta$. As shown in Fig. 9 (c, d), linear fits in log–log space confirm clear power-law behavior for both layout and cousin scaling, with strong Pearson correlations.

Benchmarking overall generalization. We compare our strongest policy (PPO-UrbanVerse), trained on all 160 UrbanVerse scenes, against foundation models MBRA (Hirose et al., 2025), CityWalker (Liu et al., 2025), S2E (He et al., 2025), and a PPO policy trained on 160 UrbanSim PG scenes, all evaluated on CraftBench. As an overfitting reference, we also train policies directly on each test scene. As shown in Tab. 3, PPO-UrbanVerse, despite its simple architecture, consistently outperforms all baselines, achieving a **+6.3%** SR gain over the second-best model MBRA. Policies trained directly on test scenes perform poorly on altered routes, revealing strong overfitting and underscoring the need for diverse training scenes to enable true generalization.

4.3 ZERO-SHOT SIM-TO-REAL POLICY TRANSFER

Zero-shot transfer across urban spaces and embodiments. We evaluate our strongest policy, trained on all UrbanVerse scenes, in 16 unseen real-world urban scenarios averaging 24.6 m per route (see Fig. 23 for examples). The same policy is deployed on two embodiments: the COCO wheeled delivery robot (Coco Robotics, 2024) and the Unitree Go2 quadruped (see Fig. 26 for robot configuration). We benchmark against navigation foundation models NoMad (Sridhar et al., 2024), S2E, and a PPO policy trained on PG scenes. Each evaluation is repeated three times, with distance-to-goal (DTG) also reported. As shown in Tab. 4, PPO-UrbanVerse significantly outperforms

Method	SR \uparrow	CT \downarrow	RC \uparrow
MBRA	35.6	25.6	52.9
CityWalker	29.2	38.2	48.6
S2E	33.1	27.7	55.7
PPO-UrbanSim	9.1	31.5	19.4
PPO-UrbanVerse	41.9	35.5	62.4
Overfitting	26.5	32.2	40.6

Table 3: Results on CraftBench.

	Wheeled	SR \uparrow	CT \downarrow	RC \uparrow	DTG \downarrow
NoMad	33.3	66.7	57.4	9.8	
CityWalker	25.0	75.0	42.7	12.0	
S2E	47.9	54.2	59.6	8.2	
PPO-UrbanSim	18.8	81.3	34.6	11.8	
PPO-UrbanVerse	77.1	22.9	83.4	3.6	
	Quadruped	SR \uparrow	CT \downarrow	RC \uparrow	DTG \downarrow
NoMad	37.5	62.5	54.4	12.5	
CityWalker	31.3	66.8	42.6	13.4	
S2E	58.6	41.7	71.4	6.3	
PPO-UrbanSim	18.8	81.3	29.1	15.4	
PPO-UrbanVerse	89.7	10.4	86.4	2.5	

Table 4: Real-world results.

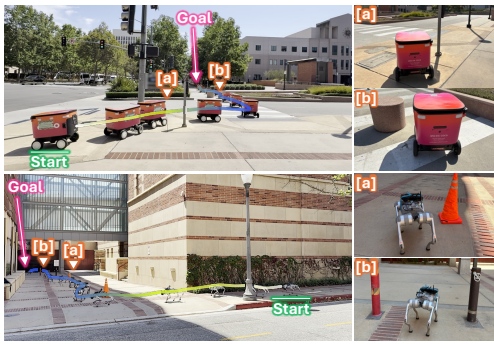


Figure 10: Visualization of real-world results.



Figure 11: Long-horizon mapless urban navigation. The PPO-UrbanVerse policy pilots the COCO robot across 337 m of public urban space, reaching the goal with only two human interventions and no collisions.

all baselines, despite its simple architecture, it surpasses the second-best model (S2E) by **+29.2%** SR on COCO and **+31.1%** SR on Go2. Foundation models like CityWalker, trained on large-scale but non-interactive data, succeed mainly in obstacle-free cases and fail when obstacles appear. In contrast, PPO-UrbanVerse consistently demonstrates robust obstacle avoidance (e.g., bypassing bollards after turns or while crossing streets). These results show that interactive capabilities learned via RL in UrbanVerse transfer effectively and reliably to real-world settings in a zero-shot manner.

Long-horizon mapless urban navigation. To stress-test policy stability, we deploy PPO-UrbanVerse on the COCO robot for a 337 m mission in real urban spaces. The robot follows GPS waypoints at 10 m intervals. For safety in public streets we implement a human–AI shared autonomy TeleOp system that allows real-time human intervention when needed. As the route recording shown in Fig. 11, it successfully completes the task with only *two* interventions. Completing such a challenging task in public streets demonstrates the robustness of policies trained on UrbanVerse scenes, a stability we attribute in part to its long training routes (≈ 200 m) that encourage generalizability for long-horizon tasks. This highlights UrbanVerse’s potential for training versatile, practical urban agents.

5 CONCLUSION

We introduce UrbanVerse, a data-driven real-to-sim system that brings our daily messy streets into interactive simulation environments. Leveraging the curated UrbanVerse-100K and the automated UrbanVerse-Gen pipeline, UrbanVerse can mass-produce simulated scenes that faithfully capture real-world distribution, enabling effective policy scaling and more generalizable urban AI embodiments.

Limitation. UrbanVerse is currently tailored to street-level urban environments; extending it to parks, campuses, or indoor–outdoor transitions would require additional terrain modeling and access structures, which we consider a promising direction for future work. In addition, our UrbanVerse-Gen real-to-sim pipeline can be affected by rare challenging video conditions—such as low light, fast motion, or heavy occlusion—that may introduce depth and pose drift or imperfect object placement.

540
541
ETHICS STATEMENT542
543
544
545
546
547
548
All city-tour videos used in this work are sourced from YouTube platforms that provide free Creative
Commons licenses. Prior to use, we apply automated and manual filtering to remove any frames
containing human faces, license plates, or other identifiable information, ensuring that no personally
sensitive data is retained. Our focus is solely on urban layouts, object distributions, and physical
attributes. While our system enables scalable simulation for embodied AI, potential misuse (*e.g.*,
surveillance applications) must be acknowledged. We therefore emphasize responsible use of our
released assets, code, and data strictly for research purposes in urban simulation and embodied AI.549
550
REPRODUCIBILITY STATEMENT
551552
553
554
555
556
557
558
To ensure reproducibility, we will release the full UrbanVerse-100K (annotated 3D assets, ground
materials, and skyboxes), the UrbanVerse-Gen implementation code, and the 160-scene UrbanVerse
library constructed from city-tour videos. All experiments are documented with dataset splits, training
details, and hyperparameters. Scripts for preprocessing, scene generation, and policy training will be
included, along with instructions for reproducing results on KITTI-360 and real-world deployment
tests. By open-sourcing our resources, we aim to support and accelerate embodied AI research in
urban environments559
560
561
562
563
564
565
566
567
568
569
570
571
572
573
574
575
576
577
578
579
580
581
582
583
584
585
586
587
588
589
590
591
592
593

594 REFERENCES
595

596 Rusul L Abduljabbar, Sohani Liyanage, and Hussein Dia. The role of micro-mobility in shaping
597 sustainable cities: A systematic literature review. *Transportation research part D: transport and*
598 *environment*, 2021. 3

599 AmbientCG. ambientcg. <https://ambientcg.com/>, 2025. 5
600

601 Jonathan Bennett. *OpenStreetMap*. Packt Publishing Ltd, 2010. 4, 21

602 Holger Caesar, Varun Bankiti, Alex H Lang, Sourabh Vora, Venice Erin Liang, Qiang Xu, Anush
603 Krishnan, Yu Pan, Giancarlo Baldan, and Oscar Beijbom. nuscenes: A multimodal dataset for
604 autonomous driving. In *CVPR*, pp. 11621–11631, 2020. 4, 21

605 Holger Caesar, Juraj Kabzan, Kok Seang Tan, Whye Kit Fong, Eric Wolff, Alex Lang, Luke Fletcher,
606 Oscar Beijbom, and Sammy Omari. nuplan: A closed-loop ml-based planning benchmark for
607 autonomous vehicles. *arXiv preprint arXiv:2106.11810*, 2021. 23

608 Devendra Singh Chaplot, Dhiraj Gandhi, Saurabh Gupta, Abhinav Gupta, and Ruslan Salakhutdinov.
609 Learning to explore using active neural slam. *arXiv preprint arXiv:2004.05155*, 2020. 3
610

611 Ziyu Chen, Jiawei Yang, Jiahui Huang, Riccardo de Lutio, Janick Martinez Esturo, Boris Ivanovic,
612 Or Litany, Zan Gojcic, Sanja Fidler, Marco Pavone, et al. Omnidre: Omni urban scene reconstruction.
613 *arXiv preprint arXiv:2408.16760*, 2024. 3

614 Bowen Cheng, Ishan Misra, Alexander G Schwing, Alexander Kirillov, and Rohit Girdhar. Masked-
615 attention mask transformer for universal image segmentation. In *CVPR*, 2022. 6
616

617 Tianheng Cheng, Lin Song, Yixiao Ge, Wenyu Liu, Xinggang Wang, and Ying Shan. Yolo-world:
618 Real-time open-vocabulary object detection. In *CVPR*, 2024. 5, 27

619 Coco Robotics. Coco Robotics, 2024. URL <https://www.cocodelivery.com/>. 9
620

621 Marius Cordts, Mohamed Omran, Sebastian Ramos, Timo Rehfeld, Markus Enzweiler, Rodrigo
622 Benenson, Uwe Franke, Stefan Roth, and Bernt Schiele. The cityscapes dataset for semantic urban
623 scene understanding. In *CVPR*, 2016. 4, 6, 21

624 Tianyuan Dai, Josiah Wong, Yunfan Jiang, Chen Wang, Cem Gokmen, Ruohan Zhang, Jiajun Wu,
625 and Li Fei-Fei. Automated creation of digital cousins for robust policy learning. In *CoRL*, 2024. 2,
626 3

627 Matt Deitke, Winson Han, Alvaro Herrasti, Aniruddha Kembhavi, Eric Kolve, Roozbeh Mottaghi,
628 Jordi Salvador, Dustin Schwenk, Eli VanderBilt, Matthew Wallingford, et al. Robothor: An open
629 simulation-to-real embodied ai platform. In *CVPR*, 2020. 23

630 Matt Deitke, Eli VanderBilt, Alvaro Herrasti, Luca Weihs, Kiana Ehsani, Jordi Salvador, Winson
631 Han, Eric Kolve, Aniruddha Kembhavi, and Roozbeh Mottaghi. Procthor: Large-scale embodied
632 ai using procedural generation. In *NeurIPS*, 2022. 3, 23

633 Matt Deitke, Rose Hendrix, Ali Farhadi, Kiana Ehsani, and Aniruddha Kembhavi. Phone2proc:
634 Bringing robust robots into our chaotic world. In *CVPR*, 2023a. 3

635 Matt Deitke, Ruoshi Liu, Matthew Wallingford, Huong Ngo, Oscar Michel, Aditya Kusupati, Alan
636 Fan, Christian Laforte, Vikram Voleti, Samir Yitzhak Gadre, et al. Objaverse-xl: A universe of
637 10m+ 3d objects. In *NeurIPS*, 2023b. 4, 22

638 Matt Deitke, Dustin Schwenk, Jordi Salvador, Luca Weihs, Oscar Michel, Eli VanderBilt, Ludwig
639 Schmidt, Kiana Ehsani, Aniruddha Kembhavi, and Ali Farhadi. Objaverse: A universe of annotated
640 3d objects. In *CVPR*, 2023c. 4, 19, 22

641 Vishnu Sashank Durbala, James F Mullen, and Dinesh Manocha. Can an embodied agent find your
642 “cat-shaped mug”? Iim-based zero-shot object navigation. *IEEE Robotics and Automation Letters*,
643 9(5):4083–4090, 2023. 33, 34

648 Alexey Dosovitskiy, German Ros, Felipe Codevilla, Antonio Lopez, and Vladlen Koltun. Carla: An
 649 open urban driving simulator. In *CoRL*, 2017. 2, 3, 23
 650

651 FreePBR. Free pbr. <https://freepbr.com/>, 2025. 5

652 Chuang Gan, Jeremy Schwartz, Seth Alter, Damian Mrowca, Martin Schrimpf, James Traer, Julian
 653 De Freitas, Jonas Kubilius, Abhishek Bhandwaldar, Nick Haber, et al. Threedworld: A platform
 654 for interactive multi-modal physical simulation. *arXiv preprint arXiv:2007.04954*, 2020. 23
 655

656 Agrim Gupta, Piotr Dollar, and Ross Girshick. Lvis: A dataset for large vocabulary instance
 657 segmentation. In *CVPR*, 2019. 4, 21

658 Honglin He, Yukai Ma, Wayne Wu, and Bolei Zhou. From seeing to experiencing: Scaling navigation
 659 foundation models with reinforcement learning. *arXiv preprint arXiv:2507.22028*, 2025. 3, 9
 660

661 Noriaki Hirose, Lydia Ignatova, Kyle Stachowicz, Catherine Glossop, Sergey Levine, and Dhruv Shah.
 662 Learning to drive anywhere with model-based reannotation. *arXiv preprint arXiv:2505.05592*,
 663 2025. 3, 9

664 Zhenling Huang, Xiaoyang Wu, Fangcheng Zhong, Hengshuang Zhao, Matthias Nießner, and Joan
 665 Lasenby. Litereality: Graphics-ready 3d scene reconstruction from rgb-d scans. *arXiv preprint*
 666 *arXiv:2507.02861*, 2025. 3

667 Jared Kaplan, Sam McCandlish, Tom Henighan, Tom B Brown, Benjamin Chess, Rewon Child, Scott
 668 Gray, Alec Radford, Jeffrey Wu, and Dario Amodei. Scaling laws for neural language models.
 669 *arXiv preprint arXiv:2001.08361*, 2020. 2

670 Bernhard Kerbl, Georgios Kopanas, Thomas Leimkühler, and George Drettakis. 3d gaussian splatting
 671 for real-time radiance field rendering. *ACM Trans. Graph.*, 42(4):139–1, 2023. 22

672

673 Eric Kolve, Roozbeh Mottaghi, Winson Han, Eli VanderBilt, Luca Weihs, Alvaro Herrasti,
 674 Matt Deitke, Kiana Ehsani, Daniel Gordon, Yuke Zhu, Kembhavi Aniruddha, Gupta Abhi-
 675 nav, and Farhadi Ali. Ai2-thor: An interactive 3d environment for visual ai. *arXiv preprint*
 676 *arXiv:1712.05474*, 2017. 3, 23

677

678 Parth Kothari, Christian Perone, Luca Bergamini, Alexandre Alahi, and Peter Ondruska. Drivergym:
 679 Democratising reinforcement learning for autonomous driving. *arXiv preprint arXiv:2111.06889*,
 680 2021. 3, 23

681 Abhinav Kumar, Yuliang Guo, Xinyu Huang, Liu Ren, and Xiaoming Liu. Seabird: segmentation in
 682 bird's view with dice loss improves monocular 3d detection of large objects. In *CVPR*, 2024. 7
 683

684 Alina Kuznetsova, Hassan Rom, Neil Alldrin, Jasper Uijlings, Ivan Krasin, Jordi Pont-Tuset, Shahab
 685 Kamali, Stefan Popov, Matteo Malloci, Alexander Kolesnikov, Tom Duerig, and Vittorio Ferrari.
 686 The open images dataset v4: Unified image classification, object detection, and visual relationship
 687 detection at scale. *IJCV*, 2020. 4, 21

688

689 Vincent Leroy, Yohann Cabon, and Jérôme Revaud. Grounding image matching in 3d with mast3r.
 In *ECCV*, 2024. 5, 27

690

691 Chengshu Li, Ruohan Zhang, Josiah Wong, Cem Gokmen, Sanjana Srivastava, Roberto Martín-
 692 Martín, Chen Wang, Gabrael Levine, Michael Lingelbach, Jiankai Sun, et al. Behavior-1k: A
 693 benchmark for embodied ai with 1,000 everyday activities and realistic simulation. In *CoRL*, 2023a.
 3, 23

694

695 Quanyi Li, Zhenghao Peng, Lan Feng, Qihang Zhang, Zhenghai Xue, and Bolei Zhou. Metadrive:
 696 Composing diverse driving scenarios for generalizable reinforcement learning. *TPAMI*, 2022. 3

697

698 Quanyi Li, Zhenghao Mark Peng, Lan Feng, Zhizheng Liu, Chenda Duan, Wenjie Mo, and Bolei
 699 Zhou. Scenarionet: Open-source platform for large-scale traffic scenario simulation and modeling.
 In *NeurIPS*, 2023b. 3

700

701 Yiyi Liao, Jun Xie, and Andreas Geiger. Kitti-360: A novel dataset and benchmarks for urban scene
 understanding in 2d and 3d. *TPAMI*, 45(3):3292–3310, 2022. 2, 7

702 Chendi Lin, Heshan Liu, Qunshu Lin, Zachary Bright, Shitao Tang, Yihui He, Minghao Liu, Ling
 703 Zhu, and Cindy Le. Objaverse++: Curated 3d object dataset with quality annotations. *arXiv*
 704 *preprint arXiv:2504.07334*, 2025a. 23

705 Fanqi Lin, Yingdong Hu, Pingyue Sheng, Chuan Wen, Jiacheng You, and Yang Gao. Data scaling
 706 laws in imitation learning for robotic manipulation. In *ICLR*, 2025b. 9

708 Xinhao Liu, Jintong Li, Yicheng Jiang, Niranjan Sujay, Zhicheng Yang, Juxiao Zhang, John Abanes,
 709 Jing Zhang, and Chen Feng. Citywalker: Learning embodied urban navigation from web-scale
 710 videos. In *CVPR*, 2025. 3, 9

711 Abhiram Maddukuri, Zhenyu Jiang, Lawrence Yunliang Chen, Soroush Nasiriany, Yuqi Xie, Yu Fang,
 712 Wenqi Huang, Zu Wang, Zhenjia Xu, Nikita Chernyadev, et al. Sim-and-real co-training: A simple
 713 recipe for vision-based robotic manipulation. *arXiv preprint arXiv:2503.24361*, 2025. 3

714 Mark Martinez, Chawin Sitawarin, Kevin Finch, Lennart Meincke, Alex Yablonski, and Alain
 715 Kornhauser. Beyond grand theft auto v for training, testing and enhancing deep learning in self
 716 driving cars. *arXiv preprint arXiv:1712.01397*, 2017. 23

718 Andrew Melnik, Benjamin Alt, Giang Nguyen, Artur Wilkowski, Qirui Wu, Sinan Harms, Helge
 719 Rhodin, Manolis Savva, Michael Beetz, et al. Digital twin generation from visual data: A survey.
 720 *arXiv preprint arXiv:2504.13159*, 2025. 3

721 Piotr Mirowski, Razvan Pascanu, Fabio Viola, Hubert Soyer, Andrew J Ballard, Andrea Banino,
 722 Misha Denil, Ross Goroshin, Laurent Sifre, Koray Kavukcuoglu, et al. Learning to navigate in
 723 complex environments. *arXiv preprint arXiv:1611.03673*, 2016. 3

725 NVIDIA. NVIDIA Isaac Sim, 2025. URL <https://developer.nvidia.com/isaac/sim>.
 726 2

727 Giulia Oeschger, Páraig Carroll, and Brian Caulfield. Micromobility and public transport integration:
 728 The current state of knowledge. *Transportation Research Part D: Transport and Environment*,
 729 2020. 2

730 OpenAI. Introducing GPT-4.1 in the API, 2025. URL <https://openai.com/index/gpt-4-1/>. 4, 5, 20, 21

733 Maxime Oquab, Timothée Darcet, Théo Moutakanni, Huy Vo, Marc Szafraniec, Vasil Khalidov,
 734 Pierre Fernandez, Daniel Haziza, Francisco Massa, Alaeldin El-Nouby, et al. Dinov2: Learning
 735 robust visual features without supervision. *arXiv preprint arXiv:2304.07193*, 2023. 6, 27

736 Philip Polack, Florent Altché, Brigitte d'Andréa Novel, and Arnaud de La Fortelle. The kinematic
 737 bicycle model: A consistent model for planning feasible trajectories for autonomous vehicles? In
 738 *2017 IEEE intelligent vehicles symposium (IV)*, pp. 812–818. IEEE, 2017. 33

739 PolyHaven. Poly haven hris. <https://polyhaven.com/hris>, 2025. 5

741 Alec Radford, Jong Wook Kim, Chris Hallacy, Aditya Ramesh, Gabriel Goh, Sandhini Agarwal,
 742 Girish Sastry, Amanda Askell, Pamela Mishkin, Jack Clark, et al. Learning transferable visual
 743 models from natural language supervision. In *ICML*, 2021. 2, 4, 6, 21, 27

745 Nikhila Ravi, Valentin Gabeur, Yuan-Ting Hu, Ronghang Hu, Chaitanya Ryali, Tengyu Ma, Haitham
 746 Khedr, Roman Rädle, Chloe Rolland, Laura Gustafson, et al. Sam 2: Segment anything in images
 747 and videos. *arXiv preprint arXiv:2408.00714*, 2024. 5, 27

748 Tianhe Ren, Shilong Liu, Ailing Zeng, Jing Lin, Kunchang Li, He Cao, Jiayu Chen, Xinyu Huang,
 749 Yukang Chen, Feng Yan, et al. Grounded sam: Assembling open-world models for diverse visual
 750 tasks. *arXiv preprint arXiv:2401.14159*, 2024. 7

751 John Schulman, Filip Wolski, Prafulla Dhariwal, Alec Radford, and Oleg Klimov. Proximal policy
 752 optimization algorithms. *arXiv preprint arXiv:1707.06347*, 2017. 7, 33

754 Dhruv Shah, Ajay Sridhar, Nitish Dashora, Kyle Stachowicz, Kevin Black, Noriaki Hirose, and
 755 Sergey Levine. Vint: A foundation model for visual navigation. *arXiv preprint arXiv:2306.14846*,
 2023. 2, 3

756 Ajay Sridhar, Dhruv Shah, Catherine Glossop, and Sergey Levine. Nomad: Goal masked diffusion
 757 policies for navigation and exploration. In *ICRA*, 2024. 3, 9, 33, 34
 758

759 Andrew Szot, Alexander Clegg, Eric Undersander, Erik Wijmans, Yili Zhao, John Turner, Noah
 760 Maestre, Mustafa Mukadam, Devendra Singh Chaplot, Oleksandr Maksymets, et al. Habitat 2.0:
 761 Training home assistants to rearrange their habitat. In *NeurIPS*, 2021. 23

762 Jur Van Den Berg, Stephen J Guy, Ming Lin, and Dinesh Manocha. Reciprocal n-body collision
 763 avoidance. In *ISRR*, 2011. 6
 764

765 Jianyuan Wang, Minghao Chen, Nikita Karaev, Andrea Vedaldi, Christian Rupprecht, and David
 766 Novotny. Vggt: Visual geometry grounded transformer. In *CVPR*, 2025. 7
 767

768 Wayne Wu, Honglin He, Jack He, Yiran Wang, Chenda Duan, Zhizheng Liu, Quanyi Li, and Bolei
 769 Zhou. Metaurban: An embodied AI simulation platform for urban micromobility. In *ICLR*, 2025a.
 2, 3, 23
 770

771 Wayne Wu, Honglin He, Chaoyuan Zhang, Jack He, Seth Z Zhao, Ran Gong, Quanyi Li, and Bolei
 772 Zhou. Towards autonomous micromobility through scalable urban simulation. In *CVPR*, 2025b. 2,
 3, 6, 7, 23, 35
 773

774 Ziyang Xie, Zhizheng Liu, Zhenghao Peng, Wayne Wu, and Bolei Zhou. Vid2sim: Realistic and
 775 interactive simulation from video for urban navigation. In *CVPR*, 2025. 3
 776

777 Jie Xu, Viktor Makoviychuk, Yashraj Narang, Fabio Ramos, Wojciech Matusik, Animesh Garg, and
 778 Miles Macklin. Accelerated policy learning with parallel differentiable simulation. *arXiv preprint*
 779 *arXiv:2204.07137*, 2022. 33, 34
 780

781 Yue Yang, Fan-Yun Sun, Luca Weihs, Eli VanderBilt, Alvaro Herrasti, Winson Han, Jiajun Wu, Nick
 782 Haber, Ranjay Krishna, Lingjie Liu, et al. Holodeck: Language guided generation of 3d embodied
 783 ai environments. In *CVPR*, 2024. 3
 784

785 Huangyue Yu, Baoxiong Jia, Yixin Chen, Yandan Yang, Puhao Li, Rongpeng Su, Jiaxin Li, Qing Li,
 786 Wei Liang, Song-Chun Zhu, et al. Metascenes: Towards automated replica creation for real-world
 787 3d scans. In *CVPR*, 2025. 3
 788

789 Xiang Zhang, Haojie Sun, Xiaoyang Pei, Linghui Guan, and Zihao Wang. Evolution of technology
 790 investment and development of robotaxi services. *Transportation Research Part E: Logistics and*
 791 *Transportation Review*, 188:103615, 2024. 2
 792

793 Bolei Zhou, Hang Zhao, Xavier Puig, Sanja Fidler, Adela Barriuso, and Antonio Torralba. Scene
 794 parsing through ade20k dataset. In *CVPR*, 2017. 4, 21
 795

796

797

798

799

800

801

802

803

804

805

806

807

808

809

810	APPENDIX	
811		
812		
813	A Demonstration Video and Interactive Visualization	17
814		
815	B User-side Pipeline	17
816		
817	C Details of UrbanVerse-100K Asset Database	19
818		
819	C.1 UrbanVerse-100K Statistics	19
820	C.2 Details of UrbanVerse-100K Annotation	19
821	C.3 Discussion on Asset Scale and Quality Issues of Existing Databases	22
822	C.4 Validation of Physical Attribute Annotations	24
823		
824		
825	D Details of UrbanVerse Scenes	25
826		
827	D.1 Additional Qualitative Examples of UrbanVerse Scenes	25
828	D.2 Details of UrbanVerse Scene Library Construction	25
829	D.3 Details of CraftBench Scene Creation	25
830		
831		
832	E Implementation Details of UrbanVerse-Gen Pipeline	27
833		
834	F Real-world Testing Scene Selection	27
835		
836	G Failure Case Analysis	28
837		
838	H Additional Experiments on Training Scene Horizon Length	30
839		
840		
841	I Additional Zero-shot Sim-to-real Transfer Results	31
842		
843	J Experiment Setup Details	32
844		
845	J.1 Definition of Urban Navigation Evaluation Metrics	32
846	J.2 Details of Training and Evaluation Setup	33
847	J.3 Details of Policy Learning	33
848	J.4 Robot Platform Configurations in Simulation	33
849	J.5 Robot Platform Configurations in Real-world	34
850		
851		
852	K Human Evaluation Details	35
853		
854		
855	L System Computational Analysis	36
856		
857		
858		
859		
860		
861		
862		
863		

This appendix provides additional demonstrations, visualizations, statistics, experiments, and implementation details that complement the main paper. App. A summarizes the supplementary demonstration videos and interactive visualizations. App. B presents the complete user-side pipeline for generating and using UrbanVerse simulation scenes. App. C provides extended statistics and annotation details of the UrbanVerse-100K database, together with a discussion of scale and quality issues in existing datasets and a quantitative validation of our physical attribute annotations. App. D offers further construction details for the 160-scene UrbanVerse library and the artist-designed CraftBench benchmark, along with additional qualitative examples. App. E describes implementation details of the UrbanVerse-Gen pipeline. App. F outlines the real-world testing scene selection, and App. G analyzes typical failure cases and reconstruction challenges. App. H provide additional experiments on scene horizon length. App. I reports the evaluation metrics, training and evaluation setup, policy learning details, and robot configurations in both simulation and the real world. Finally, App. K describes the human evaluation protocols and interface, and App. L presents the full computational and scalability analysis of UrbanVerse.

LLM USAGE DECLARATION

In our system, GPT-4.1 was employed as a tool for category listing from input videos (with all identity information masked) and for annotating semantic, affordance, and physical attributes of virtual 3D assets. For writing, GPT-4o was used to check grammar mistakes.

A DEMONSTRATION VIDEO AND INTERACTIVE VISUALIZATION

We highly encourage readers to watch the supplementary videos and interactive visualizations, which provide detailed demonstrations of our generated scenes, proposed asset database, and real-world navigation policy performance. The supplementary material is organized into four parts:

(1) Simulation Scene Generation Results: Side-by-side comparisons between real-world city-tour video and the corresponding digital-cousin simulation scenes generated by UrbanVerse, including examples from Beijing, Cape Town, and Los Angeles.

(2) Zero-shot Sim-to-real Generalization and Deployment Results: Demonstrations of a single policy trained on UrbanVerse scenes executing (i) street crossings, (ii) obstacle avoidance across diverse layouts, and (iii) long-horizon mapless navigation in real urban streets. *All real-world trials—across robots and scenes—use the same policy trained on the 160-scene UrbanVerse library.*

(3) UrbanVerse-100K Exploration: We first provide a clickable, web-based tool that can be opened in a browser to explore and analyze the semantic distribution of our large-scale UrbanVerse-100K. Next, we present a 360° flythrough showcasing 300+ curated 3D assets from UrbanVerse-100K, rendered together to illustrate object quality, category diversity, and metric-scale fidelity.

(4) CraftBench Flythrough Demonstration: 360° flythrough videos of each CraftBench test scene used for closed-loop evaluation.

For better visual quality, we also encourage readers to visit our [anonymous site here](#) for browsing higher resolution demonstration videos.

B USER-SIDE PIPELINE

In this section, we outline the full user-side pipeline for using the UrbanVerse simulation platform. As illustrated in Fig. 12, UrbanVerse supports both automatic generation of new simulation scenes from raw video inputs and direct use of built-in scene repositories, enabling a broad range of embodied AI applications.

Generating Custom Simulation Scenes. Users can create their own simulation environments directly from raw inputs. UrbanVerse-Gen accepts diverse sources such as YouTube city-tour videos, mobile-recorded walk-through clips, or folders of RGB frames. After providing the input, users simply use the UrbanVerse-Gen API to automatically convert the video into a fully interactive, physics-ready simulation scene. The pipeline handles all steps internally—from video normalization to

918 layout extraction and scene materialization—requiring no manual editing. UrbanVerse-Gen supports
 919 generating multiple “digital cousins” from one video.

920
Using Built-in Scene Repositories. UrbanVerse also provides two ready-to-use simulation libraries.
 921 **UrbanVerse-160** contains 160 automatically generated real-to-sim scenes extracted from city-tour
 922 videos across the world. **CraftBench** provides 10 high-fidelity artist-designed scenes for benchmarking
 923 robustness, generalization, and navigation difficulty. Both repositories can be loaded directly
 924 without running UrbanVerse-Gen.

925
Downstream Tasks Supported by UrbanVerse With either custom-generated scenes or the built-
 926 in repositories, users can seamlessly train and evaluate embodied agents. UrbanVerse supports
 927 reinforcement learning (e.g., PPO) for navigation and interaction, as well as imitation learning through
 928 expert demonstration collection via keyboard, joystick, gamepad, or VR teleoperation. The simulator
 929 also facilitates large-scale multimodal dataset collection (RGB, depth, normals, segmentation, LiDAR,
 930 and poses) for perception training. Finally, trained policies can be evaluated in closed-loop within
 931 UrbanVerse scenes and deployed to real robots for zero-shot sim-to-real transfer.

932
 933 Overall, UrbanVerse provides a practical, flexible, and complete user-side pipeline that spans real-
 934 to-sim scene generation, large-scale simulation assets, embodied task execution, and real-world
 935 deployment.

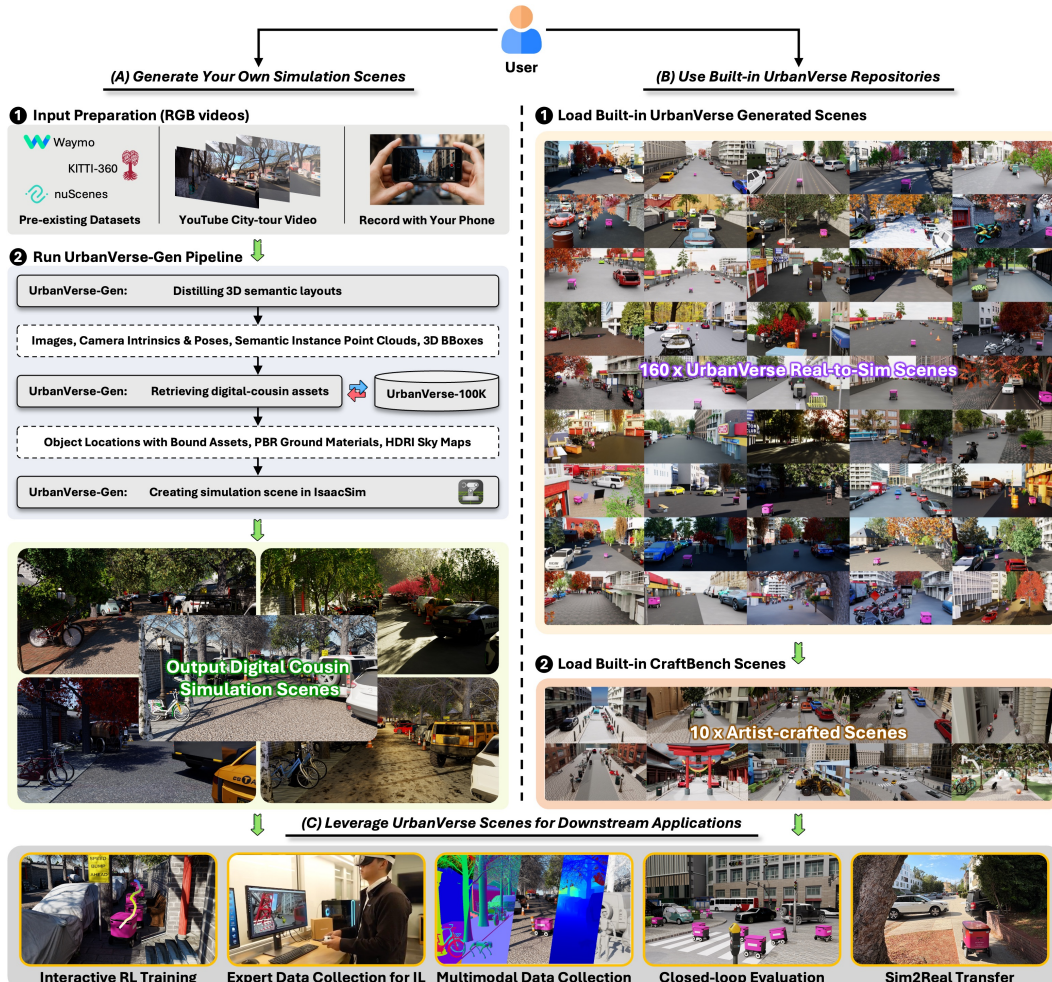


Figure 12: User-side pipeline of the UrbanVerse simulation platform.

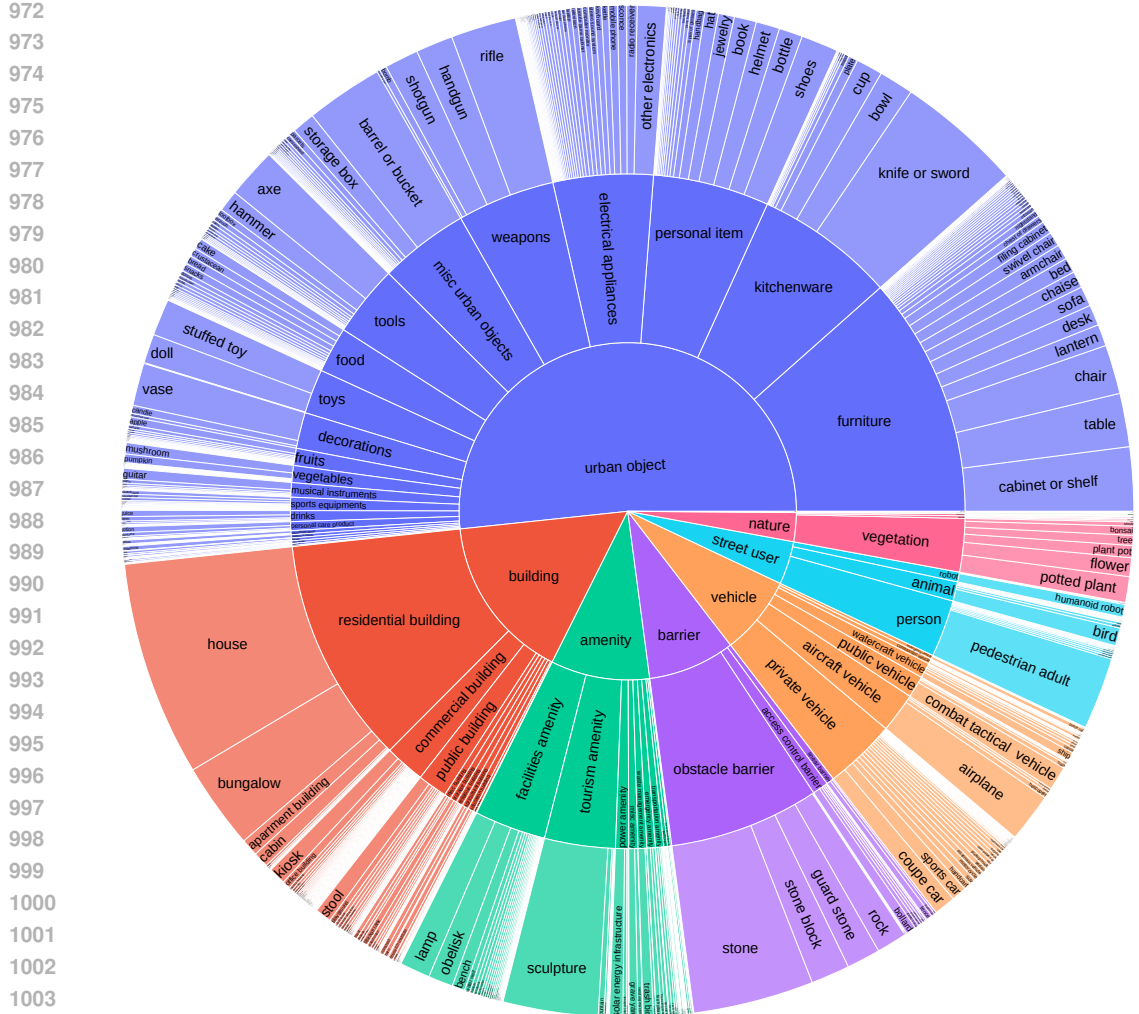


Figure 13: **Hierarchical category distribution of UrbanVerse-100K within our curated three-level urban .**

C DETAILS OF URBANVERSE-100K ASSET DATABASE

C.1 URBANVERSE-100K STATISTICS

To provide an overview of the rich semantic coverage of UrbanVerse-100K, we visualize the category distribution of its curated 102,530 object assets under our introduced three-level urban ontology.

Fig. 13 shows the hierarchical breakdown of categories across all the three levels, spanning broad groups such as *buildings*, *vehicles*, *street users*, *barriers*, *amenities*, and *urban objects*, with finer-grained divisions into 667 leaf categories. This hierarchical visualization highlights the high diversity and balance of assets across different semantic domains, ensuring comprehensive coverage of everyday urban environments.

Complementing this, Fig. 14 presents a word cloud of all 667 leaf-level categories, where font size reflects category frequency. The visualization emphasizes both common object types and rarer but important categories, demonstrating the richness and long-tailed nature of the dataset. Together, these figures illustrate the semantic diversity and scale of UrbanVerse-100K.

C.2 DETAILS OF URBANVERSE-100K ANNOTATION

Our goal is to curate a high-quality 3D urban asset database with accurate and semantically rich annotations from the 800K assets of Objaverse (Deitke et al., 2023c), thereby addressing the quality and scale issues discussed in Sec. C.3. Concretely, as described in Sec. 3.1, we design an efficient



Figure 14: Word cloud of UrbanVerse-100K category distribution over the 667 leaf-level categories.

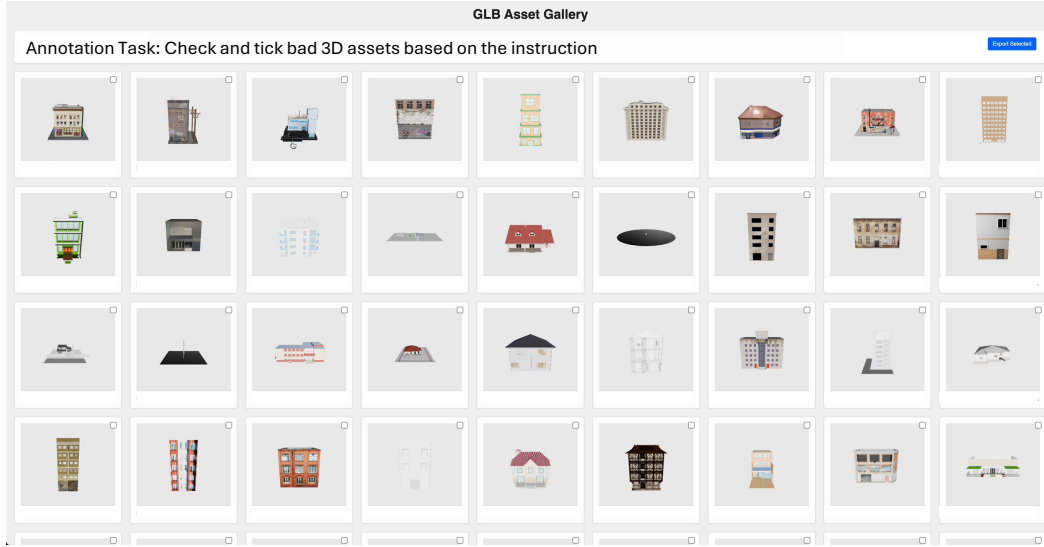


Figure 15: Efficient Three.js-based annotation interface for asset quality filtering.

semi-automatic annotation pipeline consisting of three steps: (1) *Non-simulatable asset filtering*: in-house human annotators manually remove low-quality assets that could corrupt simulation; (2) *Urban ontology and categorization*: we construct an ontology of common urban semantics and categorize assets accordingly; and (3) *Attribute annotation*: we employ GPT-4.1 ([OpenAI, 2025](#)) to automatically annotate semantic, affordance, and physical attributes of the curated assets. We now describe each step in detail.

(1) Non-simulatable asset filtering. We first eliminate assets that are likely to fail in simulation by filtering out eight common corruption types. To support this process, we built a lightweight Three.js-based GLB gallery interface that allows annotators to quickly inspect assets and perform binary quality tagging. Ten in-house annotators worked for three weeks, resulting in a curated set of 158k simulatable 3D objects. As shown in Fig. 15, our interface enables rapid quality inspection and efficient removal of unusable assets. Prior to annotation, annotators underwent training to ensure consistent identification of low-quality assets.

1080 **(2) Urban ontology and categorization.** We next construct a three-level urban ontology seeded
 1081 from the OpenStreetMap (OSM) tag structure (Bennett, 2010). OSM is a collaborative, open-source
 1082 project that provides freely accessible maps of the world, created by volunteers using GPS devices,
 1083 aerial imagery, street-level photos, and local knowledge. Its tag structure includes common urban
 1084 amenities, objects, and landmarks. Building on this structure, we expand the leaf level with categories
 1085 drawn from ADE20K (Zhou et al., 2017), Cityscapes (Cordts et al., 2016), nuScenes (Caesar et al.,
 1086 2020), LVIS (Gupta et al., 2019), and OpenImagesV7 (Kuznetsova et al., 2020). After deduplication
 1087 and refinement, the resulting ontology contains 8 top-level, 61 mid-level, and 667 leaf categories.
 1088 Assets are automatically classified into leaf classes using CLIP (Radford et al., 2021) applied to
 1089 thumbnails, followed by human verification to prune non-urban objects (e.g., weapons, spaceships)
 1090 and correct misclassifications. This process yields 102,530 assets organized under our ontology.
 1091

1092 **(3) Semantic, affordance, and physical attribute annotation.** Finally, guided by the question “How
 1093 would a robot interact with this object?”, we annotate each asset with 36 attributes spanning semantic,
 1094 affordance, and physical properties in metric units, enabling physically plausible interactions and
 1095 richer semantics. For each asset, we provide GPT-4.1 (OpenAI, 2025) with its thumbnail and four yaw
 1096 snapshots at $0^\circ/90^\circ/180^\circ/270^\circ$, prompting it to produce attribute values. This step was completed
 1097 at a total API cost of \$1,334. The exact annotation prompt is shown in Fig. 16, and the full set of
 1098 annotated attributes is presented in Fig. 17.
 1099



Figure 16: Prompt for object attribute annotation.

1134
1135
1136
1137
1138
1139
1140
1141
1142
1143
1144
1145
1146
1147
1148
1149
1150
1151
1152
1153
1154
1155
1156
1157
1158
1159
1160
1161
1162
1163
1164
1165
1166
1167
1168
1169
1170
1171
1172
1173
1174
1175
1176
1177
1178
1179
1180
1181
1182
1183
1184
1185
1186
1187

	Thumbnail	0°	90°	180°	270°
	Category Vehicle (L1) - Private Vehicle (L2) - Electric Car (L3)	Front View 180°	Wordnet pickup.n.01		
	Mass 3000 kg	Friction Coefficient 0.9	Required Force 23.5 kN	L x W x H 6.1 x 2.4 x 1.9 m	
	Young's Modulus 210 GPa	Reflectivity 0.18	Index of Refraction 1.52	Safety Clearance 1.5 m	
	Bounciness 0.05 ∈ [0, 1]	Finish Metal	Surface Roughness 0.18 ∈ [0, 1]	Surface Hardness Hard	
	Receptacle False	Support Surface False	Enterable True	Ground Mounted False	Movable True
	Affordances Drivable Openable Closable Toggleable Pressable			Traversability Obstacle	
	Interactive Parts Door Wheel Window Trunk Charging Port Mirror			Asset Quality 9 ∈ [0, 10]	
	Colors Silver Gray (85%) Black (10%) Red (3%) Yellow (2%)			Asset Composition Single	
	Materials Steel (70%) Glass (15%) Rubber (12%) Plastic (3%)			License Plate Design None	
	Description A metal, silver gray, angular electric pickup with large tinted windows and armored design				
	Manufacturer Tesla	Model Cybertruck	Emblem None	Charge Port Location Left rear quarter panel	

Figure 17: Example of full annotated attributes for each object asset in UrbanVerse-100K

C.3 DISCUSSION ON ASSET SCALE AND QUALITY ISSUES OF EXISTING DATABASES

Asset Quality Issues. High-quality 3D assets are essential for constructing realistic and physically accurate simulation environments. The recent proliferation of large-scale 3D repositories has made it possible to efficiently assemble datasets for diverse scene construction. Objaverse (Deitke et al., 2023c), for instance, provides over 800K 3D objects sourced from the Internet, and its extension Objaverse-XL (Deitke et al., 2023b) scales this collection to 10.2M unique objects from sources such as GitHub. However, because these assets are primarily scraped from the web, their quality is highly inconsistent and largely uncontrolled.

In the early stage of our project, we systematically examined Objaverse’s 800K assets and identified nine recurring forms of corruption, which affect more than half of the collection. As illustrated in Fig. 18, these issues include:

1. **Bad mesh:** incompletely reconstructed assets (often from 3D Gaussian Splatting (Kerbl et al., 2023)), resulting in noisy, broken geometry;
2. **No texture:** pure meshes without surface textures, lacking visual realism;
3. **Paper-like:** thin, hand-authored background props with negligible mesh depth, unsuitable for physical simulation;
4. **With base:** assets embedded in oversized base meshes, producing inaccurate occupancy and collisions;
5. **Terrain maps:** large terrain-like assets that cannot be meaningfully used in urban embodied AI simulation;
6. **Inconsistent names:** category names directly inherited from web tags, often written in multiple languages, idiosyncratic codes, or designer-specific terms;
7. **CAD-like:** CAD models lacking textures and physical realism, unsuitable for direct use in interactive simulation;
8. **Non-single objects:** assets that are entire scenes or contain multiple unrelated objects rather than a single entity;
9. **Non-uniform scales:** assets not in metric scale, which makes them unusable for physically grounded simulation.

The non-uniform scale issue is particularly problematic: as shown in Fig. 19, direct import of such assets can lead to absurd scenarios (e.g., a fire hydrant larger than a building). Similar issues have also

been noted in Objaverse++ (Lin et al., 2025a). To address these problems at their root, we curated a new repository, UrbanVerse-100K, by employing human annotators to carefully filter low-quality assets. This manual quality control ensures that only simulation-ready objects are included. Our curated database will be open-sourced to facilitate reliable and reproducible embodied AI research.

Asset Scale Issues. Due to these quality issues, existing simulators—such as MetaUrban (Wu et al., 2025a), UrbanSim (Wu et al., 2025b), indoor simulators (Deitke et al., 2022; Gan et al., 2020; Deitke et al., 2020; Szot et al., 2021; Kolve et al., 2017; Li et al., 2023a), and driving simulators (Dosovitskiy et al., 2017; Martinez et al., 2017; Kothari et al., 2021; Caesar et al., 2021)—typically rely on relatively small, manually curated asset repositories. Human annotators must painstakingly adjust object scales and orientations one by one, which is not scalable. As summarized in Tab. 5, current urban simulators rarely exceed 15K curated assets, limiting the diversity and richness achievable in simulation environments.

In contrast, our work introduces a hybrid annotation pipeline that combines efficient human filtering with large language model (LLM)-based automatic annotation. Human annotators perform rapid binary tagging to eliminate poor-quality assets, while LLMs contribute common-sense knowledge to automatically annotate metric scales, canonical front views, semantic categories, and physical attributes. This hybrid process enables us to construct a significantly larger, physically grounded urban asset database at scale, bridging the gap between raw Internet collections and high-quality simulation-ready repositories. In the next section, we detail our hybrid annotation pipeline.

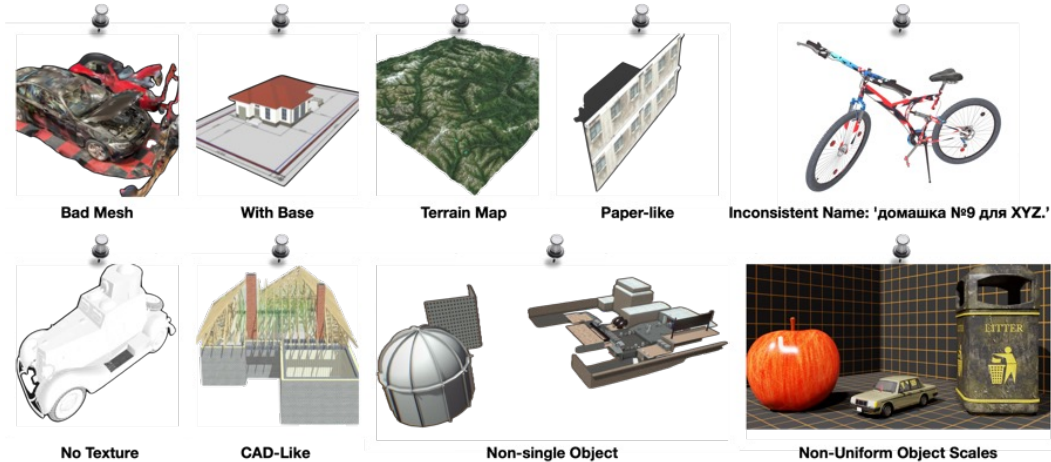


Figure 18: Typical quality issues in existing 3D asset databases.

Scenario	Simulator	Scene Creation	Physics Engine	Parallel Training	# of Scenes	# of Categories	# of Assets	Asset Physics	# of Skyboxes	# of Ground Materials
Indoor	AI2-THOR	Manual	Unity	✗	120	—	3,578	✓	✗	✗
	ProcTHOR	PG	Unity	✗	$+\infty$	108	1,633	✓	✗	✗
	Habitat 3.0	Manual	Bullet	✗	211	—	18,656	✗	✗	✗
	Holodeck	Manual	Unity	✗	$+\infty$	108	1,633	✗	✗	✗
	Behavior	Manual	PhysX	✓	50	1,900	9,000	✓	✗	✗
Driving	GAT-V	Manual	Unity	✗	—	—	✗	✗	✗	✗
	CARLA	Manual	Unreal5	✗	15	106	935	✗	1	10
	MetaDrive	PG	Panda3D	✗	$+\infty$	5	5	✗	1	3
Urban	MetaUrban	PG	Panda3D	✗	$+\infty$	39	10,000	✗	1	5
	Urban-Sim	PG	IsaacSim	✓	$+\infty$	39	15,000	✗	1	8
	UrbanVerse	Real2sim	IsaacSim	✓	$+\infty$	667	102,530	✓	306	288

Table 5: A systematic comparison of urban Embodied AI simulators.

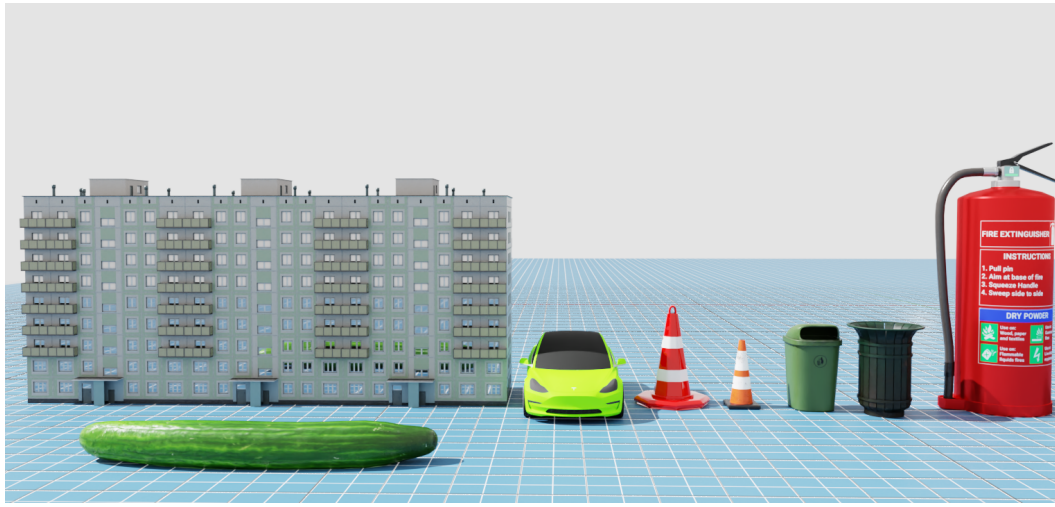


Figure 19: Non-metric scale problems in existing 3D asset databases.

Category	# Objects	MAPE H (%)	MAPE L (%)	MAPE W (%)	MAPE M (%)
Average	–	5.88 ± 3.85	6.14 ± 3.86	7.00 ± 4.11	19.58 ± 12.11
Lamborghini Huracan STO	12	0.49 ± 0.30	0.66 ± 0.40	0.51 ± 0.30	2.02 ± 1.30
McLaren 600LT Spider	4	0.59 ± 0.40	0.78 ± 0.50	0.62 ± 0.40	2.47 ± 1.50
Tesla Cybertruck	7	1.97 ± 1.40	2.50 ± 1.70	2.02 ± 1.40	9.05 ± 6.50
Land Rover Defender	2	2.99 ± 2.00	3.72 ± 2.80	1.99 ± 1.40	12.56 ± 7.50
Electric Scooter	68	5.97 ± 4.00	9.38 ± 7.00	12.32 ± 6.00	29.96 ± 19.00
Bicycle	118	7.03 ± 5.00	5.05 ± 3.00	7.75 ± 5.00	17.78 ± 13.00
Vending Machine	153	7.94 ± 5.00	9.00 ± 5.00	7.18 ± 5.00	19.60 ± 10.00
Street Cabinet	43	20.00 ± 13.00	23.00 ± 13.00	22.00 ± 12.00	14.86 ± 10.00
Parking Meter	16	7.94 ± 5.00	10.71 ± 7.00	6.56 ± 5.00	22.94 ± 14.00
Fire Hydrant	160	1.47 ± 1.00	1.53 ± 1.00	1.53 ± 1.00	7.14 ± 4.00
Traffic Cone	126	12.57 ± 9.00	20.40 ± 13.00	20.40 ± 13.00	51.07 ± 25.00
Jersey Barrier	95	5.06 ± 3.00	7.07 ± 5.00	25.83 ± 13.00	75.00 ± 50.00
Egg	188	1.09 ± 0.70	1.03 ± 0.70	1.03 ± 0.70	12.45 ± 8.00
Cigarette	28	1.00 ± 0.60	1.00 ± 0.60	1.00 ± 0.60	15.10 ± 9.00
Laptop	171	20.46 ± 13.00	5.06 ± 3.00	4.84 ± 3.00	25.02 ± 17.00
Football	99	1.50 ± 1.00	1.50 ± 1.00	1.50 ± 1.00	6.83 ± 4.00
Basketball	45	1.92 ± 1.00	1.92 ± 1.00	1.92 ± 1.00	8.97 ± 6.00

Table 6: **Evaluation of annotated physical attributes.** We report the MAPE and standard deviation against ground-truth attribute values across 17 object categories for Height (H), Length (L), Width (W), and Mass (M).

C.4 VALIDATION OF PHYSICAL ATTRIBUTE ANNOTATIONS

Validating the physical attributes annotation in UrbanVerse-100K is essential, yet direct human annotation of true object dimensions or mass is generally infeasible without expert knowledge. Prior simulators (*e.g.*, MetaUrban, UrbanSim) typically rely on *anchor-based visual calibration*, where objects are manually resized based on appearance and relative proportions. Following this practice, our main paper presents large-scale qualitative validation by placing hundreds of assets side-by-side to demonstrate consistent, physically plausible relative scales in Fig. 2.

To complement these qualitative checks, in this section, we conduct a quantitative evaluation on 17 categories comprising 1,335 objects for which reliable specifications or commonly agreed real-world dimensions are publicly available (*e.g.*, Tesla Cybertruck, vending machines, traffic cones, laptops). For each category, we compute the Mean Absolute Percentage Error (MAPE),

$$\text{MAPE} = \frac{100\%}{N} \sum_{i=1}^N \left| \frac{\text{Annotation}_i - \text{GT}_i}{\text{GT}_i} \right|,$$

over height, length, width, and mass.

1296 As summarized in Tab. 6, geometric attributes are highly accurate—typically within 1–8% MAPE
 1297 and often 1–3% for rigid objects such as cars, hydrants, and balls. Mass values exhibit larger variation
 1298 due to material uncertainty but remain within a reasonable error range (mean 19.58%). Overall, these
 1299 results demonstrate that our automatic annotation pipeline yields reliable physical attributes at scale,
 1300 enabling high-fidelity, physics-aware simulation without manual labeling.

1301 D DETAILS OF URBANVERSE SCENES

1305 D.1 ADDITIONAL QUALITATIVE EXAMPLES OF URBANVERSE SCENES

1307 Fig. 20 presents additional qualitative examples from our library of 160 automatically generated
 1308 UrbanVerse scenes. These scenes are produced by applying the full UrbanVerse-Gen pipeline to
 1309 diverse city-tour videos, capturing a wide range of real-world urban layouts, object configurations,
 1310 and appearance variations useful for embodied AI training.

1312 D.2 DETAILS OF URBANVERSE SCENE LIBRARY CONSTRUCTION

1314 **City-tour video collection.** To construct a scene library that captures diverse and realistic layouts
 1315 reflective of real-world urban settings, we collect 32 city-tour videos from YouTube released under
 1316 Creative Commons licenses. These videos span 7 continents, 24 countries, and 27 cities, providing
 1317 geographically and culturally comprehensive coverage for our city-tour video inputs. The distribution
 1318 is as follows:

- 1320 • **Continents:** Africa, Asia, Europe, Middle East, North America, Oceania, South America
- 1322 • **Countries:** Egypt, Kenya, Morocco, Nigeria, South Africa, China, India, Japan, Kazakhstan,
 1323 Singapore, South Korea, Vietnam, France, Iceland, Italy, Netherlands, Spain, Sweden, Saudi
 1324 Arabia, United Arab Emirates, Canada, Mexico, United States, Australia, New Zealand,
 1325 Argentina, Brazil, Colombia
- 1326 • **Cities:** Cairo, Nairobi, Tangier, Rabat, Lagos, Cape Town, Beijing, Shijiazhuang, New
 1327 Delhi, Tokyo, Kyoto, Almaty, Singapore, Seoul, Ho Chi Minh City, Paris, Reykjavik, Naples,
 1328 Amsterdam, Barcelona, Stockholm, Riyadh, Dubai, Toronto, Puerto Vallarta, Los Angeles,
 1329 Sydney, Auckland, Buenos Aires, São Paulo, Rio de Janeiro, Bogotá

1331 **UrbanVerse scene diversity.** Using our proposed automatic real-to-sim UrbanVerse-Gen pipeline,
 1332 we can not only mass-produce diverse scenes from collected city-tour videos but also further diversify
 1333 them through matched digital cousin object assets, ground materials, and sky maps.

1334 As illustrated in Fig. 21, each input video is reconstructed into an interactive simulation scene and
 1335 then enriched with digital cousins that introduce variation in ground conditions (*e.g.*, snow) and
 1336 illumination settings, thereby composing diverse seasonal appearances.

1338 D.3 DETAILS OF CRAFTBENCH SCENE CREATION

1340 To complement automatically generated scenes, we commission professional 3D artists to design a
 1341 suite of high-fidelity environments that serve as the CraftBench benchmark for closed-loop evaluation.
 1342 These scenes are carefully crafted to balance realism and diversity, capturing not only the everyday
 1343 orderliness of urban streets but also the messy, safety-critical edge cases that real-world agents
 1344 frequently encounter. As shown in Fig. 21, the benchmark includes diverse urban layouts such
 1345 as residential streets with garbage bags on sidewalks, narrow alleys lined with food courts, bar
 1346 streets with fallen scooters obstructing walkways, commercial districts with bike lanes, and CBD
 1347 intersections under active construction. The scenes also depict edge cases such as asymmetric
 1348 sidewalks, sidewalks blocked by illegally parked cars, and public parks populated with both dogs and
 1349 basketball courts. By combining realistic details with safety-critical anomalies, these artist-created
 scenes provide challenging yet authentic environments for evaluating embodied urban navigation.

Figure 20: **A thumbnail montage showcasing a subset of the generated UrbanVerse simulation scenes.**

1399
1400
1401
1402
1403



Figure 21: Examples of UrbanVerse scene diversity.

E IMPLEMENTATION DETAILS OF URBANVERSE-GEN PIPELINE

In this section, we provide implementation details of the proposed UrbanVerse-Gen pipeline. For structure-from-motion, we adopt MAST3R (Leroy et al., 2024) with a ViT-Large backbone to estimate camera intrinsics, metric depth, and camera poses. For 2D object semantic parsing, we use the state-of-the-art open-vocabulary detector YOLO-Worldv2 XL (Cheng et al., 2024) to obtain on-ground object bounding boxes. Subsequently, SAM 2.1 Large (Ravi et al., 2024) refines these detections by generating pixel-level semantic instance masks conditioned on the YOLO-Worldv2 predictions. To match objects with database assets, we employ CLIP ViT-L/14 (Radford et al., 2021) for textual semantic similarity, and DINOv2 ViT-B/32 (Oquab et al., 2023) to measure visual similarity between input object masks and the thumbnails of 3D assets in our database.

F REAL-WORLD TESTING SCENE SELECTION

To rigorously evaluate zero-shot sim-to-real transfer, we carefully select 16 real-world testing scenes that expose diverse challenges for two tested robot embodiments: the COCO wheeled delivery robot and the Unitree Go2 quadruped, as shown in Fig. 23. These scenarios assess each robot’s ability to follow trajectories on open ground and sidewalks, negotiate turns both with and without obstacles, and cope with safety-critical events such as obstacles appearing after sharp turns, sidewalks blocked by parked cars, and walkways cluttered with objects. Structural challenges such as narrow gates, access ramps, lampposts, and urban street crossings are also included to test mobility and

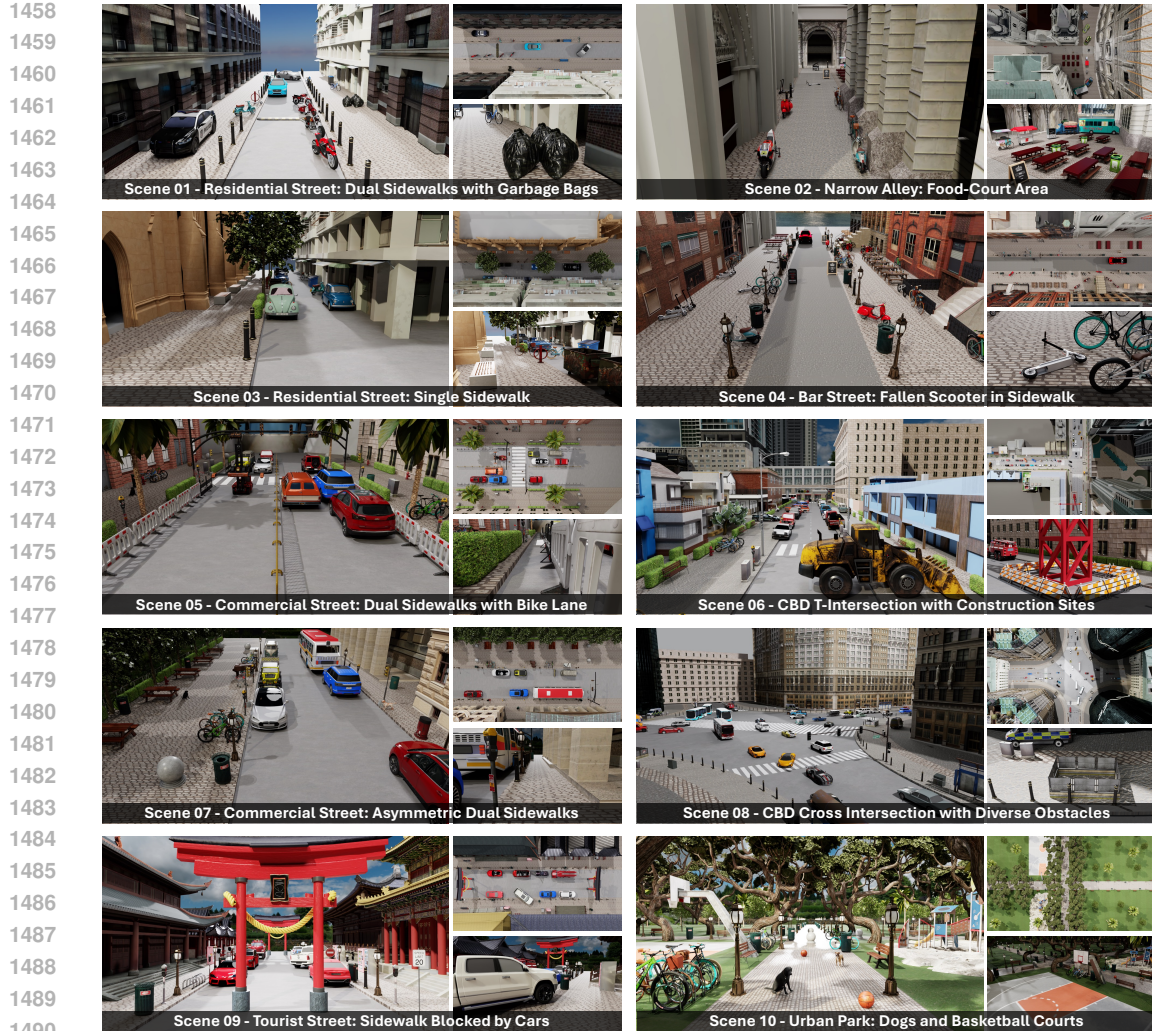


Figure 22: Examples of all CraftBench test scenes.

accessibility. Concretely, the set spans straight paths (Scenes 01, 04), turns (Scenes 02, 03, 05, 06), walkways and sidewalks with obstacles (Scenes 07, 08), obstacles appearing after turns (Scenes 09, 10), sidewalk blockage by cars (Scene 11), lampposts and plazas (Scene 12), narrow gates and ramps (Scenes 13, 14), and street crossings (Scenes 15, 16). By covering both trajectory-following and obstacle-navigation tasks across two distinct embodiments, these scenes provide a comprehensive benchmark for evaluating policy robustness and generalization in realistic urban environments.

G FAILURE CASE ANALYSIS

Challenging Input Conditions. UrbanVerse-Gen is generally robust across diverse city-tour videos, but certain input conditions can still degrade reconstruction quality. As the examples shown in Fig. 24, extremely low light, distant shot, heavy clutter, or complex terrain may affect depth estimation and geometric consistency. To prevent clearly unrecoverable clips from entering the pipeline, we screen every 10th frame with GPT-4.1 during large-scale generation and automatically filter out problematic segments.

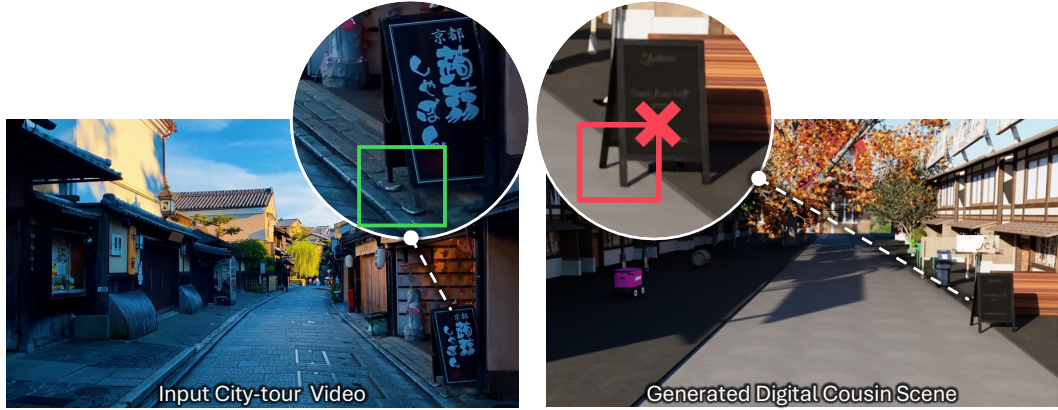
Depth and Pose Drift. Fast camera motion or unstable handheld recordings may introduce depth or pose drift, occasionally causing misplaced objects (*e.g.*, a sidewalk billboard shifted toward the roadway). Multi-view aggregation substantially reduces such errors, though they remain the most



Figure 23: **Real-world testing scenarios.** We evaluate zero-shot sim-to-real policy transfer across 16 diverse urban scenes and two embodiments (COCO wheeled delivery robot and Unitree Go2 quadruped), spanning challenges such as straight paths (Scenes 01, 04) and turns (Scenes 02, 03, 05, 06) on open ground or sidewalks, walkway and sidewalk obstacles (Scenes 07, 08), obstacles appearing after turns (Scenes 09, 10), sidewalk blockage by cars (Scene 11), structural elements including lampposts and narrow access points (Scenes 12–14), and street crossings (Scenes 15, 16). Key challenges for each scene are highlighted in Red at the upper-right corner.

common failure mode. As illustrated in Fig. 25, a sidewalk billboard shifted toward the road due to inaccurate depth and pose drift. Incorporating spatial constraints between objects and their plausible placement areas is a promising direction for further improving stability.

Imperfect Asset Retrieval. Visually complex or rare objects may not always retrieve a perfect appearance match from UrbanVerse-100K. Our three-stage matching strategy—semantic matching, geometry filtering, and appearance selection—ensures that the retrieved asset maintains correct

Figure 24: **Typical challenging input video conditions.**Figure 25: **Example failure cases from UrbanVerse-Gen.** The sidewalk billboard that is originally placed on the sidewalk in the input video is shifted toward the road due to inaccurate depth and pose drift

category, affordance, and collision geometry. As a result, appearance mismatches do not harm physical interaction and often serve as benign domain randomization.

Mis-segmentation Under Heavy Occlusion. Severe occlusion by pedestrians or vehicles can lead to incomplete masks from open-vocabulary detectors. However, because our layout extraction fuses multi-view evidence rather than relying on single-frame segmentation, the reconstructed scene geometry typically remains stable.

Impact on Downstream Learning. Despite these failure modes, we observe minimal negative impact on downstream policy learning. Multi-view fusion and strict geometry filtering provide stable scene layouts even when some frames are noisy, and both simulator evaluations and real-world sim-to-real results confirm that policies trained in UrbanVerse generalize reliably. This indicates that UrbanVerse provides sufficient scene fidelity for large-scale robot training.

H ADDITIONAL EXPERIMENTS ON TRAINING SCENE HORIZON LENGTH

In this section, we further study how the spatial horizon of training scenes affects policy learning. Specifically, we compare *Half-Length UrbanVerse scenes*, where each scene is truncated to roughly half of its original spatial extent (~ 100 m), with *Full-Length UrbanVerse scenes* that retain the complete layout (~ 200 m). Both settings use the full set of 160 UrbanVerse training scenes (320 truncated scenes in the half-length case). Policies are trained on a wheeled robot and evaluated on the ten CraftBench test scenes.

As shown in Tab. 7, full-length scenes lead to clear improvements across all metrics, raising Success Rate by +9.6, reducing Collision Time by -5.0, and increasing Route Completion by +11.6. We attribute this to two factors. First, longer scenes expose the agent to richer spatial structures, denser object configurations, and longer-range dependencies that better match the complexity of real-world navigation and the artist-designed CraftBench layouts. Second, longer episodes provide PPO with more diverse transitions and more challenging decision points per rollout, improving both collision avoidance and global route planning.

Training Scene Length	SR \uparrow	CT \downarrow	RC \uparrow
Half Length (~ 100 m)	32.3	40.5	50.8
Full Length (~ 200 m)	41.9	35.5	62.4

Table 7: **Effect of training scene horizon length.** Policies are trained on all 160 UrbanVerse scenes; the half-length setting truncates each scene to ~ 100 m, while the full-length setting uses the complete ~ 200 m layouts. Evaluation is conducted on the ten CraftBench test scenes using a wheeled robot.

These results highlight that increasing scene horizon—and thereby spatial complexity—is an effective way to improve generalization in UrbanVerse-trained policies.

I ADDITIONAL ZERO-SHOT SIM-TO-REAL TRANSFER RESULTS

We provide per-scene real-world experimental results for both robot embodiments. Specifically, Tab. 8 reports results for the COCO wheeled delivery robot, while Tab. 9 presents results for the Unitree Go2 quadruped. All experiments are conducted three times for each method.

Scene 01				Scene 02				Scene 03				Scene 04				
Route Length	22.1 m			25.8 m			22.9 m			23.1 m						
Method	SR \uparrow	CT \downarrow	RC \uparrow	DTG \downarrow	SR \uparrow	CT \downarrow	RC \uparrow	DTG \downarrow	SR \uparrow	CT \downarrow	RC \uparrow	DTG \downarrow	SR \uparrow	CT \downarrow	RC \uparrow	DTG \downarrow
NoMad	100.0	0.0	93.3	1.4	100.0	0.0	99.6	0.3	100.0	0.0	100.0	1.1	100.0	0.0	95.1	1.3
CityWalker	100.0	0.0	93.3	1.5	100.0	0.0	97.5	3.8	100.0	0.0	96.3	0.8	66.7	33.3	74.3	5.5
S2E	100.0	0.0	90.2	2.0	100.0	0.0	95.9	2.1	66.7	66.7	89.4	2.9	100.0	0.0	90.5	2.0
PPO-UrbanSim	100.0	0.0	90.9	2.0	100.0	0.0	65.0	6.0	100.0	0.0	87.1	4.3	0.0	100.0	67.3	6.0
PPO-UrbanVerse	100.0	0.0	90.9	2.0	100.0	0.0	95.1	2.1	100.0	0.0	93.1	2.0	100.0	0.0	90.7	2.0
Scene 05				Scene 06				Scene 07				Scene 08				
Route Length	13.9 m			13.7 m			24.8 m			26.2 m						
Method	SR \uparrow	CT \downarrow	RC \uparrow	DTG \downarrow	SR \uparrow	CT \downarrow	RC \uparrow	DTG \downarrow	SR \uparrow	CT \downarrow	RC \uparrow	DTG \downarrow	SR \uparrow	CT \downarrow	RC \uparrow	DTG \downarrow
NoMad	0.0	100.0	53.2	5.4	0.0	100.0	69.3	4.9	0.0	100.0	30.0	15.0	33.3	66.7	63.6	10.0
CityWalker	0.0	100.0	38.3	6.5	0.0	100.0	31.1	6.8	0.0	100.0	36.5	14.8	0.0	100.0	14.8	22.1
S2E	0.0	100.0	9.5	9.0	100.0	0.0	82.7	2.0	66.7	33.3	69.8	7.0	66.7	33.3	66.5	8.0
PPO-UrbanSim	0.0	100.0	32.5	6.8	0.0	100.0	17.3	7.9	0.0	100.0	23.5	16.3	0.0	100.0	12.5	22.8
PPO-UrbanVerse	100.0	0.0	85.6	2.1	100.0	0.0	80.4	2.1	100.0	0.0	94.2	2.0	100.0	0.0	88.1	3.1
Scene 09				Scene 10				Scene 11				Scene 12				
Route Length	36.0 m			18.9 m			22.6 m			35.7 m						
Method	SR \uparrow	CT \downarrow	RC \uparrow	DTG \downarrow	SR \uparrow	CT \downarrow	RC \uparrow	DTG \downarrow	SR \uparrow	CT \downarrow	RC \uparrow	DTG \downarrow	SR \uparrow	CT \downarrow	RC \uparrow	DTG \downarrow
NoMad	0.0	100.0	6.9	28.4	0.0	100.0	56.3	7.9	0.0	100.0	52.5	10.1	100.0	0.0	94.3	2.0
CityWalker	0.0	100.0	0.0	30.7	0.0	100.0	19.1	9.3	33.3	66.7	66.6	9.1	0.0	100.0	15.1	17.2
S2E	0.0	100.0	12.8	26.9	0.0	100.0	62.2	5.5	100.0	0.0	90.4	2.0	0.0	100.0	25.7	12.8
PPO-UrbanSim	0.0	100.0	20.9	11.8	0.0	100.0	8.4	10.6	0.0	100.0	82.9	3.5	0.0	100.0	10.0	15.0
PPO-UrbanVerse	33.3	66.7	70.2	9.1	33.3	66.7	79.4	4.0	33.3	66.7	52.4	9.7	0.0	100.0	72.9	5.3
Scene 13				Scene 14				Scene 15				Scene 16				
Route Length	28.0 m			21.8 m			25.9 m			31.7 m						
Method	SR \uparrow	CT \downarrow	RC \uparrow	DTG \downarrow	SR \uparrow	CT \downarrow	RC \uparrow	DTG \downarrow	SR \uparrow	CT \downarrow	RC \uparrow	DTG \downarrow	SR \uparrow	CT \downarrow	RC \uparrow	DTG \downarrow
NoMad	0.0	100.0	9.2	18.1	0.0	100.0	10.0	17.9	0.0	100.0	68.1	7.7	0.0	100.0	17.4	24.9
CityWalker	0.0	100.0	10.0	20.5	0.0	100.0	6.9	17.9	0.0	100.0	74.4	4.4	0.0	100.0	8.3	24.9
S2E	0.0	100.0	11.2	18.2	33.3	66.7	35.1	12.4	0.0	100.0	72.6	5.4	33.3	66.7	49.0	13.5
PPO-UrbanSim	0.0	100.0	10.7	17.6	0.0	100.0	9.2	17.4	0.0	100.0	5.0	14.9	0.0	100.0	10.5	25.2
PPO-UrbanVerse	100.0	0.0	92.7	2.1	66.7	33.3	79.6	3.9	100.0	0.0	85.8	2.1	66.7	33.3	83.9	4.6

Table 8: **Expanded real-world results of COCO wheeled robot on each scene.** Best performance is colored in Blue .

1674	Scene 01								Scene 02								Scene 03								Scene 04											
1675	Route Length	22.1 m				25.8 m				22.9 m				23.1 m				1676	Method	SR \uparrow CT \downarrow RC \uparrow DTG \downarrow				SR \uparrow CT \downarrow RC \uparrow DTG \downarrow				SR \uparrow CT \downarrow RC \uparrow DTG \downarrow				SR \uparrow CT \downarrow RC \uparrow DTG \downarrow				1677
NoMad	100.0	0.0	94.5	5.0	100.0	0.0	97.5	0.8	100.0	0.0	97.1	0.9	100.0	0.0	80.1	4.7	1678	CityWalker	100.0	0.0	94.5	5.0	100.0	0.0	96.1	1.0	100.0	0.0	98.0	0.8	100.0	0.0	90.0	5.3	1679	
S2E	100.0	0.0	88.9	2.0	100.0	0.0	93.8	2.1	100.0	0.0	92.1	2.0	100.0	0.0	68.3	6.0	1680	PPO-UrbanSim	100.0	0.0	92.3	2.0	100.0	0.0	45.6	11.4	100.0	0.0	100.0	1.5	100.0	0.0	67.1	6.1	1681	
PPO-UrbanVerse	100.0	0.0	88.7	2.1	100.0	0.0	93.9	2.0	100.0	0.0	95.2	2.1	100.0	0.0	90.3	2.0	1682																			
1683	Scene 05								Scene 06								Scene 07								Scene 08											
1684	Route Length	13.9 m				13.7 m				24.8 m				26.2 m				1685	Method	SR \uparrow CT \downarrow RC \uparrow DTG \downarrow				SR \uparrow CT \downarrow RC \uparrow DTG \downarrow				SR \uparrow CT \downarrow RC \uparrow DTG \downarrow				SR \uparrow CT \downarrow RC \uparrow DTG \downarrow				1686
NoMad	100.0	0.0	90.7	6.8	100.0	0.0	83.1	2.8	0.0	100.0	22.4	18.0	0.0	100.0	44.2	13.1	1687	CityWalker	100.0	0.0	93.0	2.4	0.0	100.0	30.8	6.0	0.0	100.0	9.1	20.7	0.0	100.0	2.7	22.8	1688	
S2E	0.0	100.0	78.5	3.3	100.0	0.0	79.0	2.1	66.7	33.3	94.6	2.1	100.0	0.0	87.0	3.1	1689	PPO-UrbanSim	0.0	100.0	15.9	8.8	0.0	100.0	65.8	3.3	0.0	100.0	30.8	15.1	0.0	100.0	14.4	20.2	PPO-UrbanVerse	
PPO-UrbanVerse	100.0	0.0	88.0	2.0	100.0	0.0	78.0	2.1	100.0	0.0	92.3	2.1	100.0	0.0	91.4	2.0	1689																			
1690	Scene 09								Scene 10								Scene 11								Scene 12											
1691	Route Length	36.0 m				18.9 m				22.6 m				35.7 m				1692	Method	SR \uparrow CT \downarrow RC \uparrow DTG \downarrow				SR \uparrow CT \downarrow RC \uparrow DTG \downarrow				SR \uparrow CT \downarrow RC \uparrow DTG \downarrow				SR \uparrow CT \downarrow RC \uparrow DTG \downarrow				1693
NoMad	0.0	100.0	74.4	10.1	0.0	100.0	83.8	13.4	0.0	100.0	36.8	13.2	0.0	100.0	18.4	18.2	1694	CityWalker	0.0	100.0	37.1	19.1	0.0	100.0	5.2	20.3	0.0	100.0	23.1	14.9	0.0	100.0	25.8	16.6	1695	
S2E	33.3	66.7	57.4	13.6	100.0	0.0	96.2	2.1	66.7	33.3	63.3	2.7	0.0	100.0	53.0	10.5	1696	PPO-UrbanSim	0.0	100.0	11.7	26.7	0.0	100.0	0.0	21.6	0.0	100.0	58.0	4.6	0.0	100.0	12.8	22.1	1697	
PPO-UrbanVerse	100.0	0.0	93.5	2.1	100.0	0.0	96.4	2.0	66.7	33.3	65.1	2.3	100.0	0.0	89.8	2.3	1697																			
1698	Scene 13								Scene 14								Scene 15								Scene 16											
1699	Route Length	28.0 m				21.8 m				25.9 m				31.7 m				1700	Method	SR \uparrow CT \downarrow RC \uparrow DTG \downarrow				SR \uparrow CT \downarrow RC \uparrow DTG \downarrow				SR \uparrow CT \downarrow RC \uparrow DTG \downarrow				SR \uparrow CT \downarrow RC \uparrow DTG \downarrow				1701
NoMad	0.0	100.0	1.5	20.8	0.0	100.0	33.6	13.9	0.0	100.0	0.0	26.4	0.0	100.0	12.2	32.4	1701	CityWalker	0.0	100.0	1.5	20.8	0.0	100.0	20.4	16.6	0.0	100.0	48.5	10.4	0.0	100.0	5.8	32.3	1702	
S2E	0.0	100.0	69.3	7.9	33.3	66.7	33.9	13.8	0.0	100.0	53.6	9.9	33.3	66.7	34.3	17.6	1703	PPO-UrbanSim	0.0	100.0	23.4	15.7	0.0	100.0	10.0	21.2	0.0	100.0	8.0	14.5	0.0	100.0	7.4	32.7	1704	
PPO-UrbanVerse	100.0	0.0	94.9	2.0	66.7	33.3	85.0	3.1	33.3	66.7	81.4	3.2	66.7	33.3	58.8	6.0	1705																			

Table 9: **Expanded real-world results of GO2 quadruped robot on each scene.** Best performance is colored in **Blue**.

J EXPERIMENT SETUP DETAILS

J.1 DEFINITION OF URBAN NAVIGATION EVALUATION METRICS

In this section, we formally define the evaluation metrics used in our urban navigation experiments.

Success Rate (SR; %). The percentage of episodes in which the robot successfully reaches the goal without collision, averaged across scenes and runs. Higher values indicate better navigation performance.

Collision Time (CT; %). The fraction of total episode time during which the robot is in contact with any obstacle. Lower values indicate safer navigation.

Route Completion (RC; %). The percentage of the planned evaluation route completed before termination (goal reached, fatal collision, off-road deviation, or timeout). Higher values reflect more reliable progress.

Distance to Goal (DTG; m). The final Euclidean distance from the robot to the goal at episode termination. Lower values indicate more precise goal reaching.

1728 J.2 DETAILS OF TRAINING AND EVALUATION SETUP
1729

1730 For training and evaluation, agents are initialized within the annotated traversable regions in Ur-
1731 banVerse scenes. The goal point is randomly sampled at a distance between 10 m and 30 m from
1732 the starting pose. Each episode runs for a fixed horizon (60s@5Hz), during which the policy must
1733 navigate toward the goal while avoiding collisions and staying within the traversable area. Rollouts
1734 are collected with a specified horizon length (*i.e.*, 32 steps) for training updates. For both training and
1735 evaluation, an episode is terminated either when the robot collides with any object in the scene or
1736 when the maximum time horizon is reached.

1737 J.3 DETAILS OF POLICY LEARNING
1738

1739 **Model architecture.** For RL training, we adopt an actor–critic architecture with continuous action
1740 space, trained using PPO (Schulman et al., 2017). Each observation is the relative position of the goal
1741 point and an RGB frame of size 135×240 with three channels. The convolutional encoder consists
1742 of three layers with depths [16, 32, 64], each followed by ReLU activation. The goal point is encoded
1743 using a MLP. No special regularization is applied. The encoder output is passed through a MLP with
1744 three hidden layers of size 128 and ELU activations. Actor and critic share the same backbone. The
1745 output distribution uses Gaussian parameters with unconstrained μ and σ , initialized respectively
1746 with the default initializer and a constant (0.0).

1747 **Reward functions.** The reward is designed to encourage goal-reaching while penalizing unsafe
1748 behaviors. Specifically:

$$1750 \quad R = R_A + R_C + R_P + R_V \quad (1)$$

- 1753 • Arrived reward R_A : A large positive reward (+2000) is given when the agent successfully
1754 reaches the goal.
- 1755 • Collision penalty R_C : A penalty (-200) is applied if the agent collides with any obstacle.
- 1756 • Position tracking R_P : A shaping reward based on the error between the commanded and
1757 actual position, with two scales: coarse (std = 5.0, weight = 10) $R_{P,c}$ and fine (std = 1.0,
1758 weight = 50) $R_{P,f}$.
- 1759 • Velocity reward R_V : A reward (weight = 10) encourages matching the target velocity
1760 command, defined as the cosine similarity between the current velocity and target velocity
1761 between the robot position and target position.

1762 This combination balances sparse terminal signals (arrival, collision) with dense shaping terms
1763 (tracking error, velocity), stabilizing training and guiding exploration.

1764 **Optimization and training hyperparameters.** We provide the detailed hyperparameters in Tab. 10.

1765 J.4 ROBOT PLATFORM CONFIGURATIONS IN SIMULATION
1766

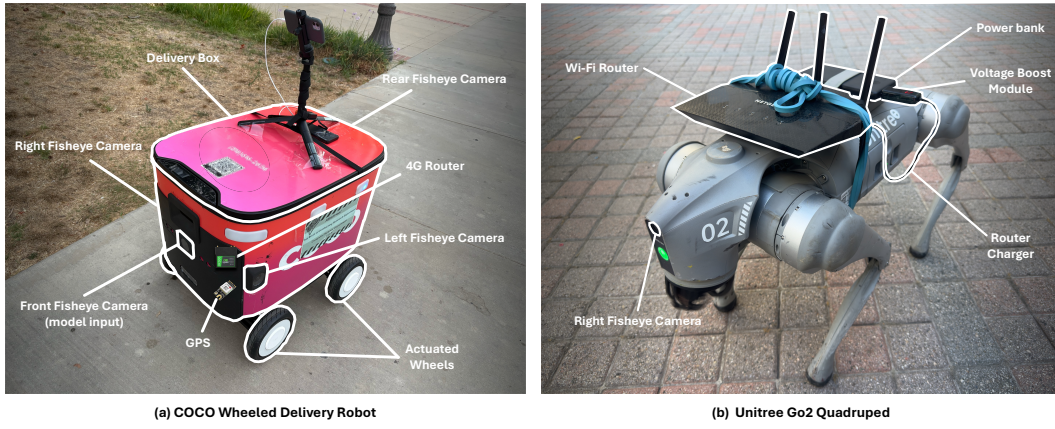
1767 Our simulated platforms are implemented in NVIDIA IsaacSim (Xu et al., 2022; Dorbala et al.,
1768 2023), a GPU-accelerated environment that provides physics-accurate interactions and photorealistic
1769 rendering. Each robot model is instantiated from its official URDF specification and equipped with
1770 RGB sensing for visual input.

1771 Locomotion is governed by a layered control architecture composed of a low-level joint controller
1772 and a high-level policy optimized through reinforcement learning. Policies are trained with Proximal
1773 Policy Optimization (PPO) (Schulman et al., 2017) under curriculum learning and terrain random-
1774 ization. The reward design promotes balance, velocity tracking, and energy-efficient movement,
1775 while penalizing collisions and falls. To enhance sim-to-real transfer, domain randomization is
1776 applied across textures, friction parameters, and mass properties. This unified framework is applied
1777 consistently across all robot embodiments, supporting scalable and embodiment-aware training.

1778 **Wheeled robot.** The wheeled platform is modeled as a differential-drive robot controlled via a
1779 kinematic formulation (Polack et al., 2017). Linear and angular velocities (v, ω) are generated from
1780 waypoints using an ideal PD controller (Sridhar et al., 2024). These commands are propagated in

Parameter	Value
Learning rate	1×10^{-4} (adaptive schedule)
Discount factor γ	0.99
GAE parameter τ	0.95
PPO clipping ϵ	0.2
KL threshold	0.01
Entropy coefficient	0.002
Critic loss coefficient	1.0
Gradient norm clipping	1.0
Horizon length	32
Minibatch size	512
Mini-epochs	5
Bounds loss coefficient	0.01
Training epochs	1500
Device	Single GPU (L40S), mixed precision

Table 10: Optimization and training hyperparameters.

Figure 26: **Robot platform configurations used in real-world experiments: (a) COCO wheeled delivery robot and (b) Unitree Go2 quadruped.**

IsaacSim’s rigid-body physics engine, where wheel-ground frictional contact governs the realized motion.

Unitree Go2 quadruped. The quadruped embodiment (Unitree Go2) is designed for agile locomotion in unstructured environments. Control actions are expressed as (v_x, v_y, ω) , again produced from waypoints through an ideal PD controller (Sridhar et al., 2024). The locomotion module itself is a compact MLP trained on IsaacSim’s standard quadruped training setups (Xu et al., 2022; Dorbala et al., 2023), enabling stable gait generation across diverse terrains.

J.5 ROBOT PLATFORM CONFIGURATIONS IN REAL-WORLD

For real-world experiments, we deploy two distinct robot platforms: the COCO wheeled delivery robot and the Unitree Go2 quadruped, as shown in Fig. 23. These platforms represent complementary embodiments for urban navigation—a compact, wheeled sidewalk delivery robot and a legged quadruped capable of traversing uneven terrain.

COCO wheeled robot. As shown in Fig. 26 (a), the real COCO robot is equipped with four actuated wheels, differential-drive odometry, a GPS unit, and multiple fisheye cameras (front, rear, left, and right) that provide panoramic perception. Its sensing and communication stack includes a 4G router for remote teleoperation connectivity and a delivery box as payload. The front fisheye camera serves

1836 as the primary input to our policy models. The robot is controlled via the same kinematic model used
 1837 in simulation, where linear and angular velocities (v, ω) are computed from waypoints using an ideal
 1838 PD controller. Odometry is used for real-time position estimation and to continuously update the
 1839 target position during navigation.

1840 **Unitree Go2 quadruped.** As shown in Fig. 26 (b), the Unitree Go2 offers a contrasting embodiment
 1841 with articulated legs and onboard compute support. It is equipped with a fisheye perception camera, a
 1842 Wi-Fi router for connectivity, and an extended power system consisting of a power bank, voltage boost
 1843 module, and router charger to support sustained experiments. Low-level locomotion is handled by
 1844 the controller provided by Unitree. Instead of executing joint-level commands from a trained policy,
 1845 we interface with the Go2 through its built-in velocity control API, sending high-level commands
 1846 (v_x, v_y, ω) that leverage its native gait generation and stability modules. LiDAR-based odometry is
 1847 used for real-time position estimation and to continuously update the target position during navigation.

1848 Together, these two platforms enable us to examine sim-to-real transfer across distinct locomotion
 1849 modalities and hardware configurations, thereby providing a broader evaluation of embodied
 1850 navigation in diverse urban settings.

1852 K HUMAN EVALUATION DETAILS

1855 **Section 1/10**

1856 **Q1: Below are three front-view images captured from different simulated urban * scenes.**

1857 **Please compare the three scenes (A, B) based on the following criteria, and choose the best one. If the difference is unclear or they are equally good, feel free to choose "Equal".**

1858 **Evaluation Criteria**

1859 **- Layout Coherence:** Which scene displays a more realistic and logically arranged layout of 3D assets, based on principles of real-world urban planning and spatial organization? Consider object alignment, spacing, and how naturally the environment flows.

1860 **- Object Diversity:** Which scene includes a more varied and representative set of urban objects, contributing to the richness, completeness, and authenticity of the environment? Layout Coherence

1861 **- Overall Urban Scene Realism:** Which scene best resembles a believable real-world urban scenario overall? Consider the combined effects of asset appropriateness, layout coherence, object diversity, and visual realism.

1862 

1863 **A is best B is best Equal**

1864 **Object Diversity**

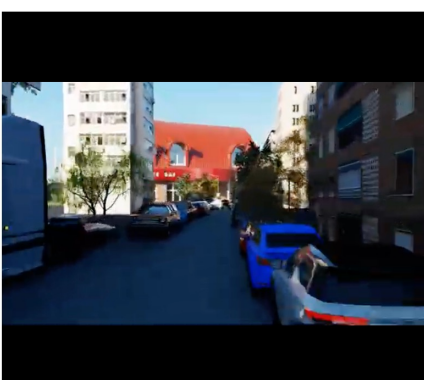
1865 **Layout Coherence**

1866 **Overall Realism**

1867 (a) User Preference Study

1868 **Scene 2/36**

1869 **Please click to play and watch the video first**

1870 

1871 **Q2: How would you rate the quality of this digital simulated urban scene in terms * of Overall Urban Scene Realism, Asset Contextual Appropriateness, Layout Realism, and Object Diversity?**

1872 **- 1 = Very Poor**
- 2 = Poor
- 3 = Average
- 4 = Good
- 5 = Excellent

1873 **1 2 3 4 5**

1874 **Very Poor Excellent**

1875 (b) Scene Quality Rating Study

1876 Figure 27: User study interface example.

1877 To better understand how human judgments align with the realism of generated scenes, we designed
 1878 two complementary user studies using a custom-built online interface, as illustrated in Fig. 27.

1879 **Comparative User Preference Study.** For the first study, participants were presented with pairs
 1880 of static overview images randomly sampled from our dataset. Each pair consisted of one scene
 1881 generated by UrbanVerse and one procedurally generated (PG) scene using UrbanSim (Wu et al.,
 1882 2025b) built from the same UrbanVerse-100K assets. As shown in Fig. 27(a), participants compared

1890 the two scenes side-by-side and were asked to select which scene performed better (or “Equal”) across
 1891 three criteria: (1) *Object Diversity* — the richness and representativeness of included urban objects;
 1892 (2) *Layout Coherence* — the realism and logical arrangement of objects based on real-world urban
 1893 design principles; and (3) *Overall Realism* — the degree to which the scene resembled a plausible
 1894 real-world street environment. Responses were collected through a simple three-choice interface (A
 1895 better, B better, Equal) for each criterion.

1896 **Scene Quality Rating Study.** In the second study, participants evaluated scene quality through
 1897 immersive video walkthroughs. Each trial displayed a 360° simulated flythrough of a given scene, as
 1898 illustrated in Fig. 27(b). Participants were then asked to assign a quality score (1–5) reflecting overall
 1899 realism, asset contextual appropriateness, layout realism, and object diversity. The Likert-style rating
 1900 scale ranged from 1 = *Very Poor* to 5 = *Excellent*. This setup allowed participants to assess not only
 1901 static composition but also temporal and spatial coherence as the camera moved through the scene.

1902 **Study Deployment.** Both studies were conducted with 32 undergraduate participants. To ensure
 1903 fairness, all scenes and videos were shuffled randomly across participants, and instructions clarified
 1904 the evaluation criteria prior to the study. This interface design ensured consistent, criterion-driven
 1905 human judgments across both comparative and rating-based evaluations.

L SYSTEM COMPUTATIONAL ANALYSIS

1910 We provide a detailed analysis of the computational cost and scalability of UrbanVerse, covering: (i)
 1911 real-to-sim scene generation with UrbanVerse-Gen, (ii) large-scale object annotation in UrbanVerse-
 1912 100K, and (iii) a comparison with the procedural workflow of UrbanSim. Results are summarized in
 1913 Tables Tab. 11, Tab. 12, Tab. 13, and Tab. 14.

1915 Video Duration (sec)	1916 Video Length (# frames)	1917 LLM Calls	1918 Scene Generation Wall Time (sec)
10	10	4	12.38
40	40	14	114.46
80	80	27	289.80
180	180	60	1135.20

1920 Table 11: **UrbanVerse-Gen real-to-sim scene generation time with varying input video lengths on an**
 1921 **NVIDIA H100 GPU.**

1924 Setting	1925 # City-tour Videos	1926 # Cousin Scenes / Layout	1927 # Unique Layouts	1928 # Total Scenes	1929 Wall Time
1926 Single layout with 5 digital cousins	1927 1	1928 5	1929 1	1930 5	1931 18.92 min
1926 160 Scenes (1 × NVIDIA H100)	1927 32	1928 5	1929 32	1930 160	1931 10.08 hrs
1926 160 Scenes (4 × NVIDIA H100, default)	1927 32	1928 5	1929 32	1930 160	1931 1.26 hrs

1932 Table 12: **Overall computational time of UrbanVerse scene generation.**

1934 **UrbanVerse-Gen Scene Generation.** As shown in Tab. 11, the computational cost of UrbanVerse-
 1935 Gen scales almost linearly with input video length. The dominant runtime component is MAST3R-
 1936 based 3D reconstruction, while GPT-4.1 queries are kept lightweight by sampling every third frame
 1937 for object categorization. Short clips (10–40 s) require 4–14 multimodal LLM calls and 12–114 s of
 1938 processing, and longer clips (80–180 s) require 27–60 calls and 289–1135 s on a single NVIDIA H100
 1939 GPU. Using 4 H100 GPUs, the system generates 160 fully interactive scenes from 180 s city-walk
 1940 videos in 1.26 hours (Tab. 12), demonstrating strong practical scalability.

1942 **UrbanVerse-100K Asset Annotation.** The UrbanVerse-100K annotation pipeline also scales ef-
 1943 ficiently. As summarized in Tab. 13, each 3D asset is annotated with exactly one GPT-4.1 call,
 averaging 2.3 s and \$0.013 per object. Annotating the full dataset of 102,530 assets requires 65.5 hours

	# Objects	GPT-4.1 Call Counts	API Wall Clock Time	API Cost
1945	1	1	0.0003 hrs	\$0.018
1946	2	2	0.0005 hrs	\$0.029
1947
1948	102,530	102,530	65.5 hrs	\$1,334
1949	Average	1 / object	2.3 sec / object	\$0.013 / object

Table 13: **Annotation cost and runtime statistics of the UrbanVerse-100K annotation pipeline.**

of API wall time and \$1,334 in total cost, providing an economical path to large-scale semantic and physical labeling without manual intervention.

Aspect	UrbanSim	UrbanVerse
How to Add a New 3D Asset	Manual annotation (metric resizing, mass setup)	Fully automated annotation pipeline
Time to Add a New 3D Asset	~600 sec	~2.3 sec
How to Add a New Scene	Manual creation of scene templates	Automatic scene generation via UrbanVerse-Gen
Time to Create a New Scene (~200m)	~240 min	~18.9 min (NVIDIA H100)
Rendering Efficiency (RGB, Single Env, L40S)	~94 FPS	~94 FPS

Table 14: **Comparison of UrbanSim and UrbanVerse for asset creation, scene generation, and rendering efficiency.**

Comparison with UrbanSim. UrbanSim relies on procedural templates that are hand-designed by developers and require manual asset annotation. While procedural sampling itself incurs little computational cost, this workflow limits realism and diversity. As shown in Tab. 14, UrbanVerse automates both scene creation and asset annotation, reducing scene generation time from ~240 min (UrbanSim) to 18.9 min, and reducing per-object annotation time from ~600 s to 2.3 s. Both systems achieve similar rendering throughput in Isaac Sim (94 FPS), but UrbanVerse provides orders-of-magnitude higher scalability and produces scenes grounded in real-world distributions.